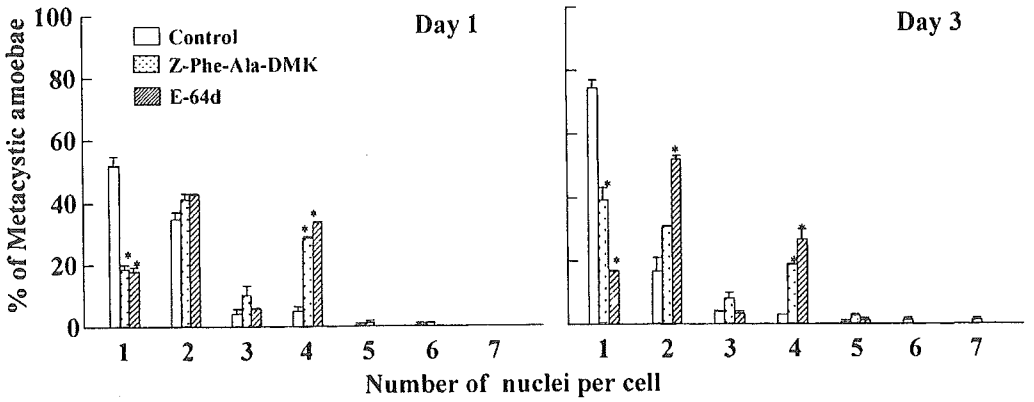

Fig. 3. The effect of cysteine protease inhibitors on the metacystic development of *E. invadens*. The cysts were transferred to a growth medium with or without 100 μM of Z-Phe-Ala-DMK or E-64d. The numbers of nuclei per metacystic amoeba stained with modified Kohn on Days 1 and 3 of incubation were counted, and the percentage of amoebae in each class (1- to 7-nucleate) was determined (each asterisk indicates $P < 0.05$).

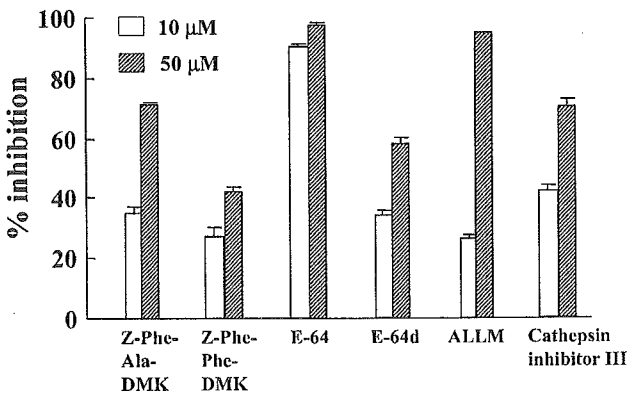

Fig. 4. The effect of cysteine protease inhibitors on cysteine protease activity in the lysates of *E. invadens* cysts. The lysates of *E. invadens* cysts (2×10^7/ml) were incubated with 10 or 50 μM each of the six inhibitors shown in Table 1. The percentages ± SE of inhibition against the control are plotted.

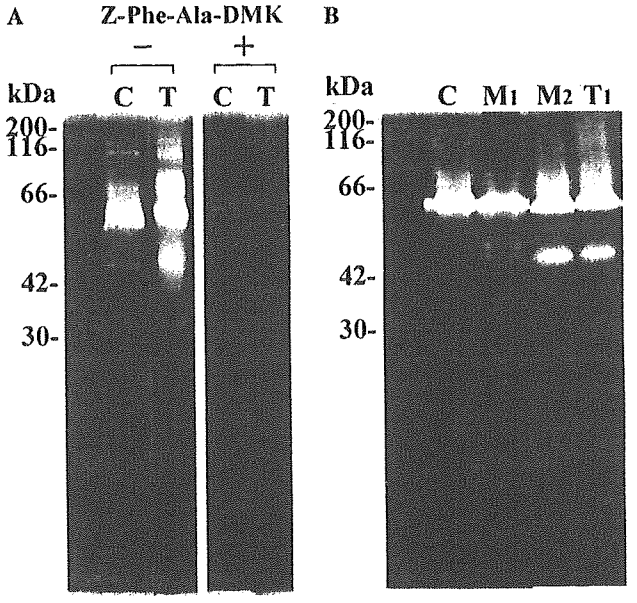

Fig. 5. Gelatin substrate SDS–PAGE of the lysates of *E. invadens* cysts, metacystic amoebae, and trophozoites. (A) Cysts (C); tophozoites (T). Following the removal of SDS, the gels were incubated in buffer alone (–) or with 1 mM Z-Phe-Ala-DMK (+). (B) M1 and M2 were metacystic amoebae from cultures with aphidicolin on Day 1, and those from cultures without the drug on Day 3, respectively. T1 was trophozoites treated similarly as those for metacystic amoebae.

cysteine protease activity in cyst lysates against synthetic peptide substrate Z-Arg-Arg-AMC was inhibited by all of the inhibitors, although there was a difference in their potency.

As shown in Fig. 5A, gelatin substrate SDS–PAGE indicated a major band of 56 kDa, broad bands of 58–66 kDa and 44–54 kDa, and a minor band of 43 kDa in cyst lysates (C). The 56 kDa band and these broad bands detected in cysts were also seen in trophozoite lysates (T). Additional broad bands of 29–41 kDa were also detected in the trophozoite lysates, suggesting a qualitative difference between these two forms. Most of these bands disappeared in the presence of Z-Phe-Ala-DMK. Newly hatched metacystic amoebae with four nuclei (M1) showed a band pattern similar to that of cysts, while more developed metacystic amoebae with one nucleus (M2) showed a band pattern similar to that of trophozoites (T1) (Fig. 5B).

4. Discussion

These results strongly suggest the participation of cysteine proteases in the excystation and metacystic development of *E. invadens*. As cyst viability was not affected by the two cysteine protease inhibitors, Z-Phe-Ala-DMK and E-64d, reduced excystation cannot be due to their toxic effect on cysts. Since other cysteine protease inhibitors used in the present study inhibited cysteine protease activity in cyst lysates, their failure to block

excystation must be due to their lower cell permeability. This is true for E-64, which had a strong inhibitory potency on the cysteine protease activity in cyst lysates. On the other hand, its inhibitory effect on excystation was much lower than E-64d, which is a membrane-permeable synthetic analog of E-64. The process of excystation includes the loosening and separation of amoeba from the cyst wall; the amoeba begins to move about within the cyst. The amoeba then flows back and forth through a small pore in the cyst wall and escapes from the cyst. Thus, cyst wall destruction is necessary for minute perforation of the cyst wall. Since the *Entamoeba* cyst wall contains a mix of protein and chitin (Arroyo-Begovich and Carbez-Trejo, 1982; Frisardi et al., 2000), it is conceivable that both protease and chitinase are essential for cyst wall destruction in the excystation process. The walls of *E. invadens* cysts are electron dense and have a uniform thickness of ~100 nm when observed by electron microscopy (Frisardi et al., 2000). Electron-dense materials were also present in the secretory vesicles and along the plasma membrane. Furthermore, the formation of a crescent-shaped space between the plasma membrane and the cyst wall was observed, and, frequently, some electron-dense bodies projected towards this newly formed space (Chavez-Munguia et al., 2003). Metacysts that endocytose the cyst wall residues were also observed. These observations suggest that secretory vesicles, including proteases and chitinase, are sent in close apposition to the plasma membrane. These enzymes are then secreted into the space between the plasma membrane and the cyst wall to destroy the cyst wall.

The hatched 4-nucleate metacystic amoeba grows rapidly and divides to form eight amoebulae. The results indicate that cysteine proteases are also involved in this metacystic development because the percentage of 4-nucleate amoebae was higher than in the controls on Day 3 of incubation. The results indicate the difference in the band pattern of protease activity between cysts and trophozoites, also changing the band pattern form from cyst-type to trophozoite-type during metacystic development. This is related to our previous results that suggest change in the expression of proteins during metacystic development (Makioka et al., 2003).

Regarding other proteases, we have previously demonstrated that lactacystin, a specific inhibitor of proteasome, had little effect on the excystation and metacystic development of *E. invadens*, suggesting the little contribution of proteasome to these processes (Makioka et al., 2002), although lactacystin inhibited the encystation in vitro of *E. invadens* (Gonzalez et al., 1999; Makioka et al., 2002).

It has recently been demonstrated that *E. histolytica* contains 20 cysteine protease (CP) genes, of which only a small subset is expressed during in vitro cultivation (Bruchhaus et al., 2003). Therefore, it is likely that at least some of these enzymes are required to infect the human host and/or complete the parasite life cycle (Bruchhaus et al., 2003). The gene that encodes CP5 is missing in the closely related but non-pathogenic *E. dispar*, suggesting the potential role of CP5 in the host tissue destruction of *E. histolytica*. Since cyst wall destruction is necessary for excystation by both amoebae, it appears that CP5 is not responsible for cyst wall destruction in either *E. histolytica* or *E. dispar*, or that other CP isoforms are used for it in *E. dispar*. Regarding CP genes in *E. invadens*, it has recently been demonstrated that among the 20 CP genes of *E. histolytica*, 14 homologous genes are found in this parasite (Wang et al., 2003).

Future study will focus on the identification and characterization of CP isoforms responsible for the excystation and metacystic development of *Entamoeba*, which will lead to a more accurate understanding of these processes and also to the identification of targets for vaccination and chemotherapy to inhibit *Entamoeba* infection.

Acknowledgments

We thank Dr. N. Watanabe for his valuable discussion with us, Dr. L. S. Diamond for supplying the *E. invadens*, and T. Yamashita and T. Tadano for their technical assistance. This work was supported by a Grant-in-Aid for Scientific Research from the Ministry of Education, Culture, Sports, and Technology of Japan, and by a Health Science Research Grant for Research on Emerging and Re-emerging Infectious Diseases from the Ministry of Health, Labor, and Welfare of Japan.

References

Arroyo-Begovich, A., Carbez-Trejo, A., 1982. Location of chitin in the cyst wall of *Entamoeba invadens* with the colloidal gold tracers. Journal of Parasitology 68, 253–258.

Bruchhaus, I., Loftus, B.J., Hall, N., Tannich, E., 2003. The intestinal protozoan parasite *Entamoeba histolytica* contains 20 cysteine protease genes, of which only a small subset is expressed during in vitro cultivation. Eukaryotic Cell 2, 501–509.

Chavez-Munguia, B., Cristobal-Ramos, A.R., Gonzalez-Robles, A., Tsutsumi, V., Martinez-Palomo, A., 2003. Ultrastructural study of *Entamoeba invadens* encystation and excystation. Journal of Submicroscopy and Cytological Pathology 35, 235–243.

Cleveland, L.R., Sanders, E.P., 1930. Encystation, multiple fission without encystment, excystation, metacystic development, and variation in a pure line and nine strains of *Entamoeba histolytica*. Archiv für Protistenkunde 70, 223–266.

Diamond, L.S., Harlow, D.R., Cunnick, C.C., 1978. A new medium for the axenic cultivation of *Entamoeba histolytica* and other *Entamoeba*. Transactions of the Royal Society of Tropical Medicine and Hygiene 72, 431–432.

Dobell, C., 1928. Researches on the intestinal protozoa of monkeys and man. Parasitology 20, 357–412.

Eichinger, D., 1997. Encystation of entamoeba parasites. Bioessays 19, 633–639.

Frisardi, M., Ghosh, S.K., Field, J., Van Dellen, K., Rogers, R., Robbins, P., Samuelson, J., 2000. The most abundant glycoprotein of amebic cyst walls (Jacob) is a lectin with five cys-rich, chitin-binding domains. Infection and Immunity 68, 4217–4224.

Garcia-Zapien, A.G., Hernandez-Gutierrez, R., Mora-Galindo, J., 1995. Simultaneous growth and mass encystation of *Entamoeba invadens* under axenic conditions. Archives of Medical Research 26, 257–262.

Geiman, Q.M., Ratcliffe, H.L., 1936. Morphology and life-cycle of an amoeba producing amoebiasis in reptiles. Parasitology 28, 208–230.

Gonzalez, J., Bai, G., Frevert, U., Corey, E.J., Eichinger, D., 1999. Proteasome-dependent cyst formation and stage-specific ubiquitin mRNA accumulation in *Entamoeba invadens*. European Journal of Biochemistry 264, 897–904.

Keene, W.E., Petitt, M.G., Allen, S., McKerrow, J.H., 1986. The major neutral proteinase of *Entamoeba histolytica*. Journal of Experimental Medicine 163, 536–549.

Kumagai, M., Kobayashi, S., Okita, T., Ohtomo, H., 2001. Modifications of Kohn's chlorazol black E staining and Wheatley's trichrome staining for temporary wet mount and permanent preparation of *Entamoeba histolytica*. Journal of Parasitology 87, 701–704.

Laemmli, U.K., 1970. Cleavage of structural proteins during the assembly of the head of bacteriophage T4. Nature 227, 681–685.

López-Romero, E., Villagómez-Castro, J.C., 1993. Encystation in *Entamoeba invadens*. Parasitology Today 9, 225–227.

Makioka, A., Kumagai, M., Ohtomo, H., Kobayashi, S., Takeuchi, T., 2002. Effect of proteasome inhibitors on the growth, encystation, and excystation of *Entamoeba histolytica* and *Entamoeba invadens*. Parasitology Research 88, 454–459.

Makioka, A., Kumagai, M., Kobayashi, S., Takeuchi, T., 2003. *Entamoeba invadens*: inhibition of excystation and metacystic development by aphidicolin. Experimental Parasitology 103, 61–67.

McConnachie, E.W., 1955. Studies on *Entamoeba invadens* Rodhain, 1934, in vitro, and its relationship to some other species of *Entamoeba*. Parasitology 45, 452–481.

McKerrow, J.H., 1989. Parasite proteases. Experimental Parasitology 68, 111–115.

Que, X., Reed, S.L., 2000. Cysteine proteinases and the pathogenesis of amebiasis. Clinical Microbiology Review 13, 196–206.

Rengpien, S., Bailey, G.B., 1975. Differentiation of *Entamoeba*: a new medium and optimal conditions for axenic encystation of *E. invadens*. Journal of Parasitology 61, 24–30.

Rosenthal, P.J., 1999. Proteases of protozoan parasites. Advanced Parasitology 43, 106–139.

Sajid, M., McKerrow, J.H., 2002. Cysteine proteases of parasitic organisms. Molecular and Biochemical Parasitology 120, 1–21.

Sanchez, L., Enea, V., Eichinger, D., 1994. Identification of a developmentally regulated transcript expressed during encystation of *Entamoeba invadens*. Molecular and Biochemical Parasitology 67, 125–135.

Sharma, M., Hirata, K., Herdman, S., Reed, S., 1996. *Entamoeba invadens*: characterization of cysteine proteinases. Experimental Parasitology 84, 84–91.

Shaw, M.K., Roos, D.S., Tilney, L.G., 2002. Cysteine and serine protease inhibitors block intracellular development and disrupt the secretary pathway of *Toxoplasma gondii*. Microbes and Infection 4, 119–132.

Wang, Z., Samuelson, J., Clark, C.G., Eichinger, D., Paul, J., Dellen, K.V., Hall, N., Anderson, I., Loftus, B., 2003. Gene discovery in the *Entamoeba invadens* genome. Molecular and Biochemical Parasitology 129, 23–31.

Available online at www.sciencedirect.com
SCIENCE DIRECT®
ELSEVIER
Molecular & Biochemical Parasitology 145 (2006) 216–225
MOLECULAR & BIOCHEMICAL PARASITOLOGY

Characterization of protein geranylgeranyltransferase I from the enteric protist *Entamoeba histolytica*☆

Asao Makioka[a], Masahiro Kumagai[a], Tsutomu Takeuchi[b], Tomoyoshi Nozaki[c,d,*]

[a] *Department of Tropical Medicine, Jikei University School of Medicine, 3-25-8 Nishi-shinbashi, Minato-ku, Tokyo 105-8461, Japan*
[b] *Department of Tropical Medicine and Parasitology, Keio University School of Medicine, 35 Shinanomachi, Shinjuku-ku, Tokyo 160-8582, Japan*
[c] *Department of Parasitology, Gunma University Graduate School of Medicine, 3-39-22 Showa-machi, Maebashi, Gunma 371-8511, Japan*
[d] *Precursory Research for Embryonic Science and Technology, Japan Science and Technology Agency, 2-20-5 Akebonocho, Tachikawa, Tokyo 190-0012, Japan*

Received 23 August 2005; received in revised form 28 September 2005; accepted 4 October 2005
Available online 19 October 2005

Abstract

Entamoeba histolytica is a unique protozoan parasite possessing both protein farnesyltransferase and geranylgeranyltrasferase I (GGT-I) for isoprenylation of small GTPases. In this study, we demonstrated unique enzymological properties of the amebic GGT-I (*Eh*GGT-I), including substrate specificity and insensitivity to known mammalian inhibitors. Some of important residues of the catalytic β subunit implicated in the specificity for GTPase acceptors and prenyl donors are substituted in *Eh*GGT-I. Recombinant α and β subunits of *Eh*GGT-I, co-expressed in *Escherichia coli*, showed activity to transfer geranylgeranyl to both human wild-type (CVLS) and mutant (CVLL) H-Ras, while the mammalian GGT-I geranylgeranylated, but not farnesylated, only mutant H-Ras. All the representative amebic Ras and Rho/Rac small GTPases with phenylalanine, leucine, methionine, or alanine terminus were preferentially geranylgeranylated by *Eh*GGT-I. This indicates that the acceptor specificity of the amebic GGT-I is remarkably broader than that of its mammalian counterpart. In contrast to *Eh*FT, which farnesylates but not geranylgeranlylates solely *Eh*Ras4-CVVA, *Eh*GGT-I also showed significant farnesyltransferase activity against Ras GTPase acceptors. *Eh*GGT-I showed remarkable resistance to peptidomimetics known to inhibit mammalian GGT-I. Together with our previous observation that this parasite does not appear to depend on farnesylation for a majority of Ras and Rho/Rac, these data indicate that biological and biochemical advantages leading to the evolutional selection of this isoprenyl modification must exist uniquely in this parasitic protist. Finally, remarkable biochemical differences in binding to substrates and inhibitors between amebic and mammalian GGT-I highlight this enzyme as an attractive target for the development of new chemotherapeutics against amebiasis.

Keywords: *Entamoeba histolytica*; Protein prenylation; Protein geranylgeranyltransferase I; Protein farnesyltransferase; Ras superfamily small GTPases

1. Introduction

Protein geranylgeranyltransferase type I (GGT-I; E.C. 2.5.1.59) and a closely related protein, farnesyltransferase (FT), are prenyl enzymes responsible for geranylgeranylation and farnesylation, respectively, which are major posttranslational lipid modifications of proteins including small GTPases of the Ras superfamily [1]. The isoprenylation of small GTPases is required for membrane association and their function in signal transduction involved in cell proliferation, differentiation and intracellular membrane trafficking [1–3]. GGT-I and FT, which are also called as CaaX prenyltransferases [4], catalyze

Abbreviations: GGT-I, protein geranylgeranyltrasferase I; *Eh*GGT-I, *Entamoeba histolytica* GGT-I; FT, protein farnesyltransferase; GGPP, geranylgeranyl pyrophosphate; FPP, farnesyl pyrophosphate; GGT-Iα, α subunit of GGT-I; GGT-Iβ, β subunit of GGT-I; SDS-PAGE, sodium dodecyl sulfate-polyacrylamide gel electrophoresis; NTA, Ni-nitrilotriacetic acid

☆ *Note:* The nucleotide sequence data of *Entamoeba histolytica* GGT-Iβ reported in this paper has been submitted to the DDBJ/GenBank®/EBI data bank with Accession number AB161971.

* Corresponding author. Tel.: +81 27 220 8020; fax: +81 27 220 8025.
E-mail address: nozaki@med.gunma-u.ac.jp (T. Nozaki).

0166-6851/$ – see front matter © 2005 Elsevier B.V. All rights reserved.
doi:10.1016/j.molbiopara.2005.10.005

the transfer of the geranylgeranyl and farnesyl group from geranylgeranyl pyrophosphate (GGPP) and farnesyl pyrophosphate (FPP), respectively, to the cysteine residue of a carboxyl-terminal CaaX of small GTPases including Ras, Rac, Rho, and Rap, where C, a, or X is cysteine, an aliphatic amino acid, or any amino acid, respectively. Mammalian FT or GGT-I generally prefers substrates including small GTPases possessing a terminal CaaX, where X is one of the following amino acids: Cys, Ser, Gln, Ala, Met, Thr, His, Val, Asn, Phe, Gly, or Ile for FT and Leu, Phe, Ile, Val, or Met for GGT-I in the order of decreasing affinity [5]. However, exceptions have been described in various organisms: e.g. K-RasB-CVIM is isoprenylated by both FT and GGT-I [6]. These data suggest the presence of not-yet-identified mechanistic details determining the substrate preferences of these isoprenyl enzymes. The third enzyme, GGT-II, transfers the geranylgeranyl groups from GGPP to both cysteine residues of CC- or CXC-containing proteins almost exclusively composed of members of the Rab family small GTPases [1].

Mutations in Ras, which correlate with cellular transformation and tumor development, have been found in nearly 30% of all human cancers [7]. Oncogenic Ras proteins have been shown to require farnesylation for their ability to transform cells [1]. Consequently, FT has been attracting attention as a target of cancer chemotherapy [8]. FT inhibitors have also been found to be effective against parasitic infections such as African sleeping sickness caused by *Trypanosoma brucei* and malaria caused by *Plasmodia* species [9]. Although GGT-I has drawn less attention than FT, GGT-I inhibitors are also viewed as potential anticancer agents because K-RasB, the most commonly mutated form of Ras, has often been shown to be geranylgeranylated as well as farnesylated [6]. Furthermore, a number of studies have shown that GGT-I inhibitors are effective against tumor progression [10] and smooth muscle hyperplasia [11].

Entamoeba histolytica is the intestinal protozoan parasite that causes amebic dysentery, colitis, and liver abscess in humans, and is responsible for an estimated 50 million cases of amebiasis and 40–100 thousand deaths annually [12]. A number of small GTPases of this parasite have been studied including Ras/Rap [13,14], Rho/Rac [15–19], and Rab [20–23], and the molecular and cellular functions of some of these small GTPases are beginning to be unveiled [13,18,19,23–25]. To elucidate the prenylation of these small GTPases in *E. histolytica*, we previously cloned genes encoding the α- and β-subunits of FT of this parasite and characterized the FT recombinant enzyme, which revealed remarkable biochemical differences in binding to substrates and inhibitors from mammalian FT [26]. We showed that the amebic FT did not utilize a majority of Ras and Rap as a substrate, but specifically farnesylated only a single Ras isotype, Ras4, which possesses an unusual primary structure. However, the molecular and biochemical identity of an enzyme (or enzymes) responsible for the isoprenylation of the remaining Ras and Rap proteins in this organism remains unknown.

To better understand the peculiarity of substrate selection of isoprenylation enzymes in this parasitic protozoon, we characterized GGT-I from *E. histolytica* (*Eh*GGT-I) in this study. We show that *Eh*GGT-I exhibits activity against a wide spectrum of small GTPases of *E. histolytica*, which is in marked contrast to *Eh*FT. We also show remarkable differences in substrate specificity and sensitivity against known peptidomimetic inhibitors of mammalian GGT-I between *Eh*GGT-I and rat GGT-I, indicating amebic GGT-I to be an ideal target for the development of new chemotherapeutics against amebiasis.

2. Materials and methods

2.1. Parasite

Trophozoites of *E. histolytica* strain HM:IMSS cl6 [27] were cultured axenically in BI-S-33 medium at 35.5 °C [28].

2.2. Chemicals

Recombinant rat GGT-I, recombinant human H-Ras-CVLS (wild type), H-Ras-CVLL (mutant), and peptidomimetic inhibitors GGTI-287 (*N*-4-[2 (*R*)-amino-3-mercatopropyl] amino-2-phenylbenzoyl-(L)-leucine trifluoroacetate) and GGTI-297 (*N*-4-[2(*R*)-amino-3-mercatopropyl]amino-2-naphthylbenzoyl-(L)-leucine trifluoroacetate) were purchased from EMD Biosciences (La Jolla, CA). [^{3}H] geranylgeranyl pyrophosphate (23.0 Ci/mmol) and [^{3}H] farnesyl pyrophosphate (16.1 Ci/mmol) were purchased from Perkin-Elmer Life Sciences (Boston, MA). Restriction endonucleases and modifying enzymes were purchased from Takara Biochemical (Tokyo, Japan). The other chemicals and reagents were purchased from either Sigma–Aldrich Fine Chemicals (St. Louis, MO) or Wako Pure Chemical Industries (Osaka, Japan) unless otherwise mentioned and were of the highest purity available.

2.3. cDNA library of E. histolytica

A trophozoite cDNA library of *E. histolytica* was constructed using the poly(A)$^+$ RNA and λZAP II phage (Stratagene, La Jolla, CA) as described previously [29].

2.4. Identification and cloning of GGT-Iβ of E. histolytica

We designed oligonucleotide primers to amplify the protein-coding region of the GGT-I β subunit from *E. histolytica* by PCR based on a homology search using yeast and mammalian GGT-I against the *E. histolytica* genome database available at The Institute for Genomic Research (http://www.tigr.org/tdb/). The sense and antisense primers for *Eh*GGT-Iβ were 5′-ATGAATGCACCTAATTTAAGAAGTGAAG-3′ and 5′-TCAAAGATATGATGGTTTTTCAATTCC-3′, respectively. PCR was performed using a one-hundredth volume of the cDNA phage lysate as a template with the following parameters. The initial step of denaturation at 94 °C for 3 min was followed by 30 cycles of denaturation at 94 °C for 1 min, annealing at 55 °C for 2 min, and extension at 72 °C for 2 min. The final step at 72 °C for 10 min was added to complete the extension. The amplified DNA fragments were electrophoresed, purified using a Geneclean II kit (BIO101, La Jolla, CA) and used as templates for subsequent PCR (see below). Since FT and GGT-I share their α subunit in all the organisms so far analyzed, we utilized the α subunit of

E. histolytica FT [26] as the GGT-I α subunit. Thus, the term "GGT-I α subunit" is synonymous with "FT α subunit" in this study. The nucleotide sequences reported in this paper have been submitted to the DDBJ/GenBank™/EBI Data Bank with accession number AB161971 (GGT-Iβ of *E. histolytica*).

2.5. Construction of a plasmid to express recombinant EhGGT-I

A plasmid containing the protein-coding regions of GGT-Iα (without the stop codon), GGT-Iβ (with the stop codon), and the ribosome-binding sequence (GAGGAGTTTTAACTT) between them was constructed by three rounds of PCR [30,31]. Briefly, a set of initial-round PCRs were conducted to amplify the GGT-Iα and GGT-Iβ protein-coding region using a sense primer, 5′-ATGGAAGAAGACGAAGAAATCACATTTG-3′, and an antisense primer, 5′-ATGATTAGTAATTTTTGTTAAATACCAATCCC-3′ (for GGT-Iα), and using a sense primer, 5′-ATGAATGCACCTAATTTAAGAAGTGAAG-3′, and an antisense primer, 5′-TCAAAGATATGATGGTTTTTCAATTCC-3′ (for GGT-Iβ), respectively. The second PCR was conducted using the respective product of the first reaction as a template. To amplify the GGT-Iα protein-coding region (excluding the stop codon) flanked by a *Bam*HI site (italicized) and the ribosome-binding site (underlined), a sense primer, 5′-GGA*GGATCC*CATGGAAGAAGACGAAGAAATCACATTTG-3′ (primer 1) and an antisense primer, 5′-AAGTTAAAACTCCTCATGATTAGTAATTTTTGTTAAATACCAATCCC-3′ were used. To amplify the GGT-Iβ sequence including the stop codon, flanked by the ribosome-binding site (underlined) and a *Hin*dIII site (italicized), a sense primer, 5′-GAGGAGTTTTAACTTATGAATGCACCTAATTTAAGAAGTGAAG-3′, and an antisense primer, 5′-CCA*AAGCTT*TCAAAGATATGATGGTTTTTCAATTCC-3′ (primer 2), were used. The third round of PCR was conduced using a mixture of the products of the second round, and primers 1 and 2. The resulting 2-kb PCR product was digested with *Bam*HI and *Hin*dIII and ligated into *Bam*HI, and *Hin*dIII double-digested pQE31 (QIAGEN, Hilden, Germany) to construct pEhGGT-Iαβ. Nucleotide sequences were confirmed with an ABI Prism BigDye terminator cycle sequencing ready reaction kit (PE Applied Biosystems, Foster City, CA) on an ABI Prism 310 Genetic Analyzer. In pEhGGT-Iαβ, the GGT-Iα and GGT-Iβ protein-coding regions placed in tandem were presumably translationally coupled, facilitating the co-expression of these two subunits at similar levels. An amino-terminal histidine tag was also engineered in pEhGGT-Iα to facilitate purification.

2.6. Construction of plasmids to express recombinant small GTPases

Construction of plasmids for *Eh*Rasl-4 and *Eh*RacC were previously described [26]. Similarly, a protein-coding region of *Eh*RacA, *Eh*RacG, and *Eh*Rapl-2 flanked by additional *Bam*HI and *Sal*I sites (italicized) were amplified by PCR using cDNA as a template and the following sense and antisense primers: 5′-GGA*GGATCC*CATGCAAGCTGTCAAATGTGT-3′ and 5′-CCAGT*CGAC*TTAGAATAATAAACATCCTCT-3′ (*Eh*RacA); 5′-GGA*GGATCC*CATGAGACCAGTGAAACTTGT-3′ and 5′-CCA*GTCGAC*TTAGAATAATGAGCATCCTTT-3′ (*Eh*RacG); 5′-GGA*GGATCC*CATGCCAGTAAAAGACTATAAAATTGTAGTA-3′ and 5′-CCA*GTCGAC*TTAGAGAAGAGAACAATGATGAGCATGATC-3′ (*Eh*Rapl); 5′-GGA*GGATCC*CATGCCAGTGAAAGACTACAAAATTGTAGTA-3′ and 5′-CCA*GTCGAC*TTAGAAGAGAGAACATCCACCACTCTTCTT-3′ (*Eh*Rap2), where the restriction sites are italicized. PCR products were electrophoresed, purified, and cloned into *Bam*HI, and *Sal*I double-digested pQE31 plasmid to obtain pEhRacA, pEhRacG, pEhRapl and pEhRap2. The resulting plasmids were designed to express proteins containing an amino-terminal histidine tag to facilitate purification.

2.7. Expression and purification of recombinant proteins

Plasmids constructed as described above were introduced into *Escherichia coli* M15 cells. A 12 ml seed culture was grown overnight at 37 °C in LB medium containing 100 μg/ml ampicillin and 25 μg/ml kanamycin. The overnight culture was then inoculated into 250 ml of fresh medium containing the antibiotics. The bacteria were grown for 1 h, and then for another 4 h after the addition of 1 mM isopropyl β-D-thiogalactopyranoside to induce protein expression. The bacteria were harvested by centrifugation at 4000 × *g* for 20 min, and the pellet was stored at −20 °C until purification. The recombinant proteins were purified according to the manufacturers' instructions. Briefly, the bacterial cells were resuspended in cold lysis buffer, phosphate-buffered saline (PBS), pH 8.0, containing 10 mM imidazole and 1% lysozyme, sonicated, and centrifuged at 10,000 × *g* for 20 min. The supernatant was applied to a Ni-NTA agarose column (QIAGEN), washed extensively with the wash buffer containing 20 mM imidazole, and eluted with the lysis buffer containing 250 mM imidazole. The purified recombinant GGT-I and small GTPase proteins were then dialyzed against the enzyme assay buffer described below and 40 mM Tris–HCl, pH 8, containing 90 mM NaCl, 10 mM $MgCl_2$ and 2 mM dithiothreitol (DTT) and stored with 20 and 50% glycerol, respectively, at −80 °C until use. After purification, recombinant *Eh*GGT-I was estimated to be >95% pure by densitometric quantitation. Protein concentrations were determined by the method of Bradford [32] using Protein Assay CBB solution (Nacalai Tesque, Kyoto, Japan). Bovine serum albumin was used as the protein standard.

2.8. Sequence analysis

GGT-Iβ and FTβ protein sequences from *E. histolytica* and 16 other organisms were retrieved from the databases available at TIGR and the National Center for Biotechnology Information (http://www.ncbi.nih.gov/) using the BLASTP and TBLASTN algorithms. The protein alignment and phylogenetic analyses were performed with CLUSTAL W version 1.81 [33] using the Neighbor-joining (NJ) method [34] with the Blosum matrix created using the CLUSTAL W program [33]. Unrooted NJ trees

were drawn with TreeView version 1.6.0 [35]. Branch lengths and bootstrap values (1000 replicates) [36] were derived from the NJ analysis.

2.9. Protein analyses

The expression and purity of recombinant proteins were evaluated by standard sodium dodecyl sulfate-polyacrylamide gel electrophoresis (SDS-PAGE) as described [37]. To prepare *E. histolytica* extracts, trophozoites were washed three times with ice cold PBS, resuspended at 10^7 ml^{-1} in PBS containing a proteinase inhibitor cocktail [1 mM phenylmethylsulfonyl fluoride, 1 nM trypsin inhibitor, 100 μM trans-epoxysuccinyl-L-leucylamino-(4-guanidino) butane, 1 μg/ml pepstatin A, 1 μg/ml leupeptin, 1 μg/ml *N*-α-p-tosyl-L-lysine chloromethyl ketone hydrochloride, and 1 mM benzamidine hydrochloride], and subjected to three cycles of freezing and thawing. After centrifugation at 10,000 × *g* for 10 min, the supernatant was subjected to further analyses.

2.10. Immunoblot analysis

SDS-PAGE was conducted using 4 μg each of recombinant *Eh*GGT-I, *Eh*FT, and recombinant rat GGT-I. Polyclonal antiserum against recombinant *Eh*GGT-I was commercially raised in a rabbit by Takara-Bio (Ohtsu, Japan) by four injections of 0.8 mg of the purified recombinant protein with Freund's complete and incomplete adjuvant at 2-week intervals. Two weeks after the last immunization, the immune serum was collected. Immunoblot analysis was performed as described [37] using primary antibodies at 1:100 and peroxidase-conjugated anti-rabbit IgG antibody (ICN-Cappel, Cappel, OH) at 1:1000. The blots were visualized with 4-chloro-l-naphthol and hydrogen peroxide.

2.11. Enzyme assays

The enzymatic activity of recombinant GGT-I and the whole lysate of *E. histolytica* trophozoites were assayed by measuring the incorporation of [^{3}H] GGPP or [^{3}H] FPP into the recombinant small GTPases of *E. histolytica*, human H-Ras-CVLL, or H-Ras-CVLS. The assay was performed essentially as described previously [38] with minor modifications. Briefly, in standard assays, the reaction mixture contained, in a total volume of 50 μl, 50 mM HEPES, pH 7.5, 5 mM $MgCl_2$, 25 μM $ZnCl_2$, 5 mM DTT, 0.1% PEG 20,000, 130 nM [^{3}H] GGPP (3 μCi/ml) or 187 nM [^{3}H] FPP (3 μCi/ml), 1.8 μg (1.8 μM) of the acceptor, and 2.4 μg (0.6 μM) of the purified recombinant GGT-I or 140 μg of the *E. histolytica* lysate. The reaction was initiated by the addition of either the recombinant enzyme or cell extracts, was run at 30 °C for 20 min, and terminated by the addition of 200 μl of 10% HCl in ethanol. The quenched reactions were allowed to stand at room temperature for 15 min. After the addition of 200 μl of 100% ethanol, the reactions were vacuum-filtered through a glass filter GF/C (Whatman, Maidstone, UK) using a Sampling Manifold (Millipore Corporation, Bedford, MA). The filters were washed with 4 ml of absolute ethanol, and then subjected to scintillation counting (LS 6000IC, Beckman Coulter, Fullerton, CA). The K_m values were calculated from Lineweaver–Burk plots. GGT-I assays were also conducted in the presence of known peptidomimetic inhibitors of GGT-I (GGTI-287 and GGTI-297) under the conditions described above.

3. Results

3.1. Features of GGT-Iβ from E. histolytica

A nucleotide sequence of *Eh*GGT-Iβ obtained by PCR was identical to the sequence available from the genome database (40.m00215). The predicted protein-coding region of *Eh*GGT-Iβ, consisting of 1014 bp, encodes a protein of 337 amino acids with a calculated molecular mass of 38.2 kDa and a p*I* of 6.71. A search for previously identified domains and motifs [39] using the NCBI Conserved Domain Search revealed that *Eh*GGT-Iβ possessed one CAL1 domain and two "prenyltransferase and squalene oxidase repeats" (Fig. 1). The deduced protein sequence of *Eh*GGT-Iβ was aligned with those of other organisms using the CLUSTAL W program (Fig. 1). *Eh*GGT-Iβ is the smallest in size, and apparently lacks the secretory signal sequence, organelle targeting signals, and domains implicated in membrane association including the transmembrane domain and myristoylation signal. *Eh*GGT-Iβ revealed a 22–30% positional identity with the GGT-Iβ of *Saccharomyces cerevisiae*, *Caenorhabditis elegans*, *Drosophila melanogaster*, *Homo sapiens*, or *Arabidopsis thaliana*. Among 12 residues implicated in making contact with peptide substrates in mammalian GGT-Iβ [40], four important residues Ala^{123}, Met^{124}, Arg^{202}, and Leu^{320} in *Hs*GGT-Iβ, were replaced by Ser^{107}, Tyr^{108}, Ser^{189}, and Met^{304}, respectively, in *Eh*GGT-Iβ, (Fig. 1). Furthermore, among 17 residues implicated in making contact with isoprenoid in mammalian GGT-Iβ [40], five residues, Phe^{52}, Thr^{127}, Cys^{177}, Phe^{324}, and Asn^{345} of *Hs*GGT-Iβ, were replaced by Met^{47}, Ala^{111}, Ser^{164}, Cys^{308}, and Il^{329}, respectively, in *Eh*GGT-Iβ (Fig. 1). All three residues implicated in the interaction with zinc in the catalytic center of mammalian GGT-Iβ [40] were conserved in *Eh*GGT-Iβ.

3.2. Phylogenetic analysis of EhGGT-Iβ and EhFTβ

A phylogenetic tree of GGT-Iβ and FTβ from *E. histolytica* and other organisms was constructed (Fig. 2). The β subunit of GGT-I and FT formed statistically significant (i.e. supported with 100% bootstrap proportion) well-separated clades, suggesting that the separation of GGT-I and FT occurred prior to the separation of these species. The β subunit of amebic GGT-I is divergent from those from all the other organisms including mammals; the overall shapes of these two trees are, however, significantly different. These results indicate that the catalytic β subunits of *Eh*FT and *Eh*GGT-I evolved independently to gain phylogenetic positions well separate from other eukaryotes, consistent with the presence of the unique biochemical properties of *Eh*GGT-I (see below).

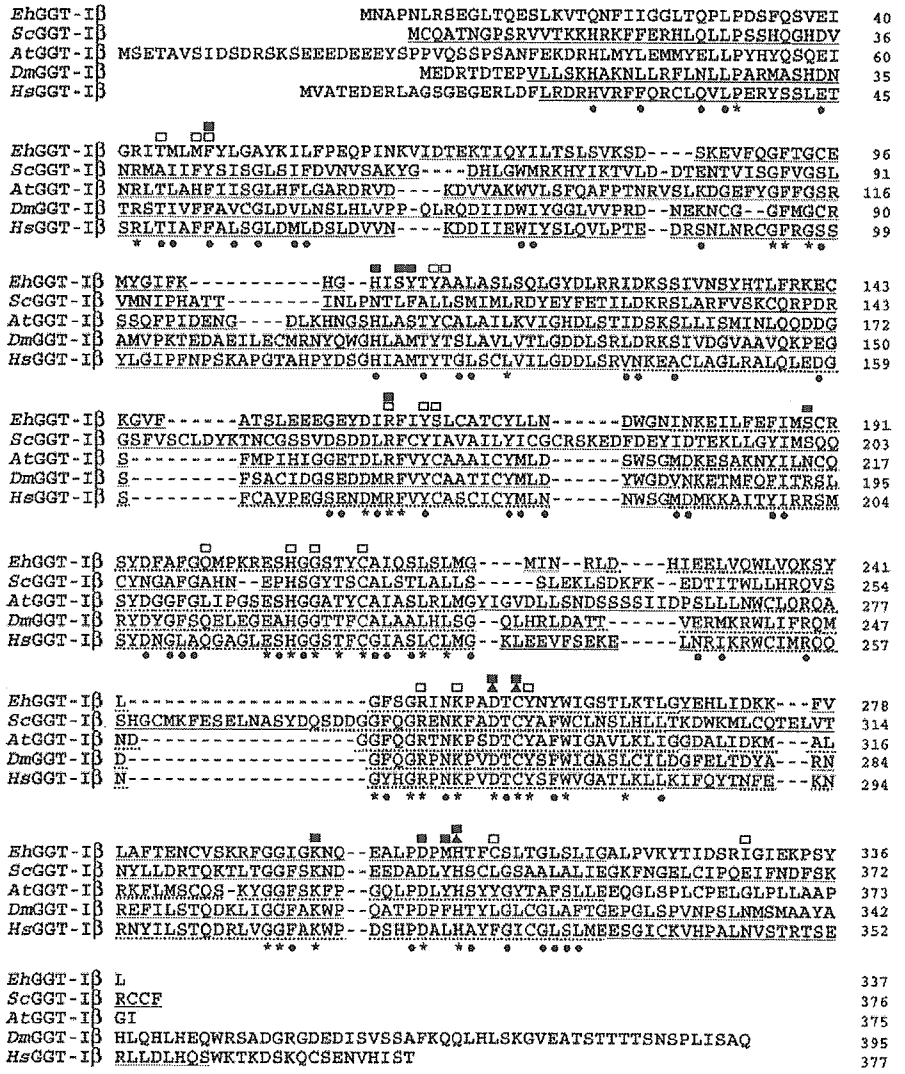

Fig. 1. Alignment of the deduced amino acid sequences of the β subunit of protein geranylgeranyltransferase I from *Entamoeba histolytica* and other organisms. *Eh, E. histolytica; Sc, Saccharomyces cerevisiae; At, Arabidopsis thaliana; Dm, Drosophila melanogaster; Hs, Homo sapiens*. The *asterisks* (*) under the alignments indicate identical amino acid residues and the *dots* (●) indicate conserved amino acid substitutions. CAL1 domains detected by the NCBI Conserved Domain Search are *underlined* (partially *dotted-underlined*). The prenyltransferase/squalene oxidase repeats, also detected by the search, are *dotted-underlined*. Amino acids implicated in the binding of isoprenoids or peptide substrates [40] are marked with *open* or *filled squares*, respectively. Amino acids implicated in the coordination of zinc are marked with *filled triangles*. DDBJ/EMBL/GeneBank™ accession numbers are given in Fig. 2.

3.3. Demonstration of GGT activity of the recombinant EhGGT-I against human Ras proteins

*Eh*GGT-Iα, identical to the previously characterized *Eh*FTα [26], and *Eh*GGT-Iβ were co-expressed in *E. coli*, and the complex was co-purified as described in Section 2. The purified complex revealed two major proteins of an equal intensity with an apparent molecular mass of 38 and 36 kDa on SDS-PAGE analysis (Fig. 3). Although the apparent molecular mass of the recombinant α subunit agreed well with the theoretical value of 37.6 kDa (of the native protein) with the amino- and carboxyl-terminal addition of Met-Arg-Gly-Ser-His-His-His-His-His-His-Thr-Asp-Pro and Gly-Gly-Phe, respectively, β subunit of 36 kDa was smaller than the theoretical value of 38.2 kDa for *Eh*GGT-Iβ. The molecular identity of these two subunits was confirmed using immunoblot analysis (see below). Densitometric quantitation of these two bands also supported the premise that they contain an equal number of protein molecules (data not shown). Thus, the recombinant *Eh*GGT-Iα and *Eh*GGT-Iβ were present as a stable complex with a stoichiometric ratio of 1:1 in the process of purification by Ni-nitrilotriacetic acid (NTA) agarose (Fig. 3). A rabbit antiserum raised against the recombinant *Eh*GGT-I reacted with both the α and β subunits of *Eh*GGT-I and the α subunit of *Eh*FT, but neither with the β subunit of *Eh*FT nor rat GGT-I (Fig. 3B and C). These data confirmed the identity of *Eh*GGT-Iα

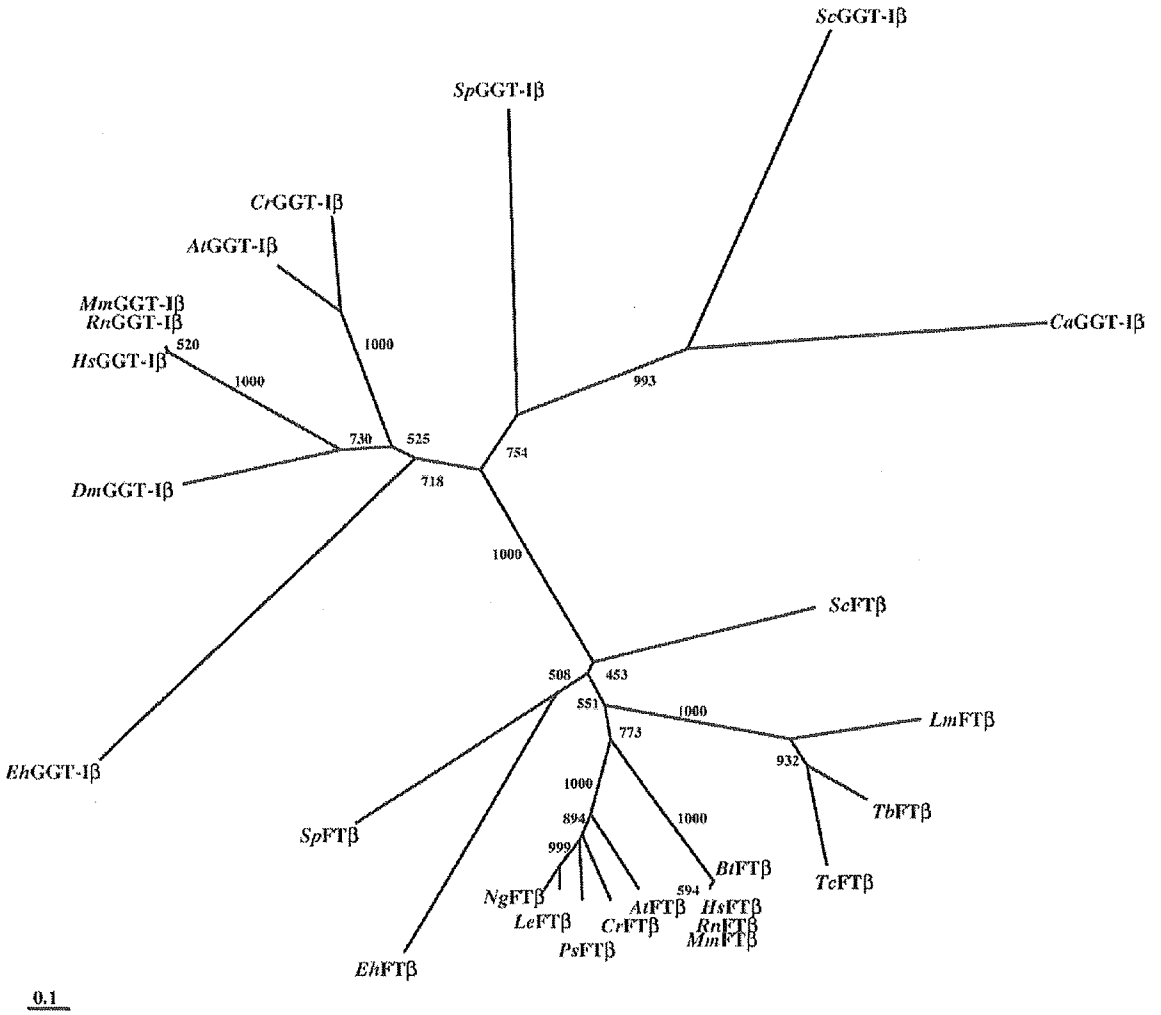

Fig. 2. Phylogenetic tree of the β subunits of GGT-I and FT. The tree was constructed by neighbor-joining distance analysis using the CLUSTAL W and TreeView programs. Line lengths indicate distances between nodes. The bar represents a distance of 0.1 amino acid change per site. Bootstrap values for 1000 replicates are shown at the nodes. Abbreviations are: *Eh, E. histolytica* (DDBJ/EMBL/GeneBank™ number of FTβ and GGT-Iβ, BAC98942, AB161971); *Sc, S. cerevisiae* (P22007, P18898); *Sp, Schizosaccharomyces pombe* (013782, P32434); *Tb, Trypanosoma brucei* (AAF73920, none); *Tc, T. cruzi* (AAL69905, none); *Lm, Leishmania major* (AAL69907, none); *At, A. thaliana* (AAF74564, NP_81487); *Ng, Nicotiana glutinosa* (AAB38796, none); *Ps, Pisum sativum* (Q04903, none); *Le, Lycopersicon esculentum* (AAC49666, none); *Cr, Catharanthus roseus* (AAQ02809, AAP50511); *Ca, Candida albicans* (none, AAD32539); *Dm, D. melanogaster* (none, AAC46972); *Mm, Mus musculus* (NP_666039, NP_766215) *Rn, Rattus norvegicus* (Q02293, P53610); *Bt, Bos taurus* (P49355, none); *Hs, H. sapiens* (NP_002019, NP_005014).

and *Eh*GGT-Iβ to the two corresponding bands on SDS-PAGE. They also suggest that antigenicity differed between the β subunits of *Eh*GGT-I and *Eh*FT and between *Eh*GGT-I and rat GGT-I.

Recombinant *Eh*GGT-I showed comparable GGT activity against both wild-type human recombinant H-Ras-CVLS [1.36 ± 0.028 (mean ± standard deviation of the mean) nmol GGPP/mg protein] and mutant H-Ras-CVLL (1.65 ± 0.013 nmol GGPP/mg protein), whereas rat GGT-I showed activity of a similar level against H-Ras-CVLL (1.83 ± 0.162), but no detectable activity against H-Ras-CVLS (Fig. 4), suggesting the presence of marked differences in acceptor specificity between *E. histolytica* and rat GGT-I.

3.4. Specificities of EhGGT-I for acceptors and prenyl donors

We further examined the acceptor (i.e. protein substrate) specificity of *Eh*GGT-I toward amebic small GTPases, *Eh*Ras, *Eh*Rac, and *Eh*Rap. We tested if *Eh*GGT-I utilizes a limited range of substrates among possible small GTPases, as previously demonstrated for *Eh*FT, which showed very strict substrate specificity predominantly against *Eh*Ras4-CVVA [26]. The recombinant *Eh*GGT-I showed GGT activity toward all the tested *Eh*Ras proteins: *Eh*Rasl-CIMF, *Eh*Ras2-CELL, *Eh*Ras3-CSVM, and *Eh*Ras4-CVVA, with *Eh*Ras2 being the best substrate (Fig. 4). Notable differences in GGT-I activity exist depending upon the Ras species. For example, GGT-I activity

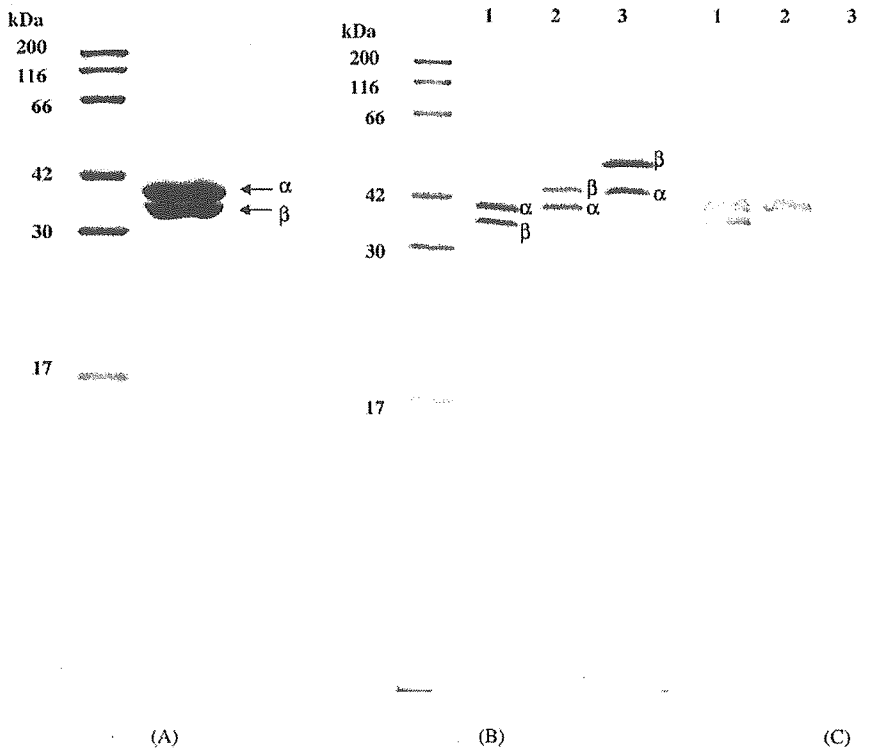

Fig. 3. SDS-PAGE and immunoblot analyses of the purified recombinant GGT-I of *E. histolytica*. (A) *Eh*GGT-1α and β subunits were coexpressed in *Escherichia coli* and purified on Ni-NTA agarose. The samples were subjected to SDS-PAGE and stained with Coomassie Brilliant Blue. (B) Approximately 4 μg each of recombinant *Eh*GGT-I (*Lane* 1), *Eh*FT (*Lane* 2) and rat GGT-I (*Lane* 3) were subjected to SDS-PAGE and stained with Coomassie Brilliant Blue. (C) The same samples in (B) were subjected to SDS-PAGE, transferred, and immunostained with rabbit antiserum against recombinant. *Eh*GGT-I.

toward *Eh*Ras2-CELL was >100 times higher than *Eh*Ras3-CSVM. The recombinant *Eh*GGT-I also transferred geranylgeranyl to *Eh*RacA-CLLF, *Eh*RacC-CALL, *Eh*RacG-CSLF, *Eh*Rapl-CSLL, and *Eh*Rap2-CSLF (Fig. 4). In contrast, rat GGT-I revealed comparable activity against *Eh*RacA-CLLF, *Eh*RacG-CSLF; however, rat GGT-I showed almost no detectable activity against the other three *Eh*Ras proteins and significantly lower activity against *Eh*RacC-CALL, *Eh*Rapl-CSLL, and *Eh*Rap2-CSLF. We also assayed for GGT activity in the whole lysate of the *E. histolytica* trophozoites. GGT activity (4.9–9.4 pmol GGPP/mg protein) was detected against *Eh*Ras 1-4 and human H-Ras-CVLL in the whole lysate, verifying the presence of GGT activity against these representative Ras proteins (data not shown).

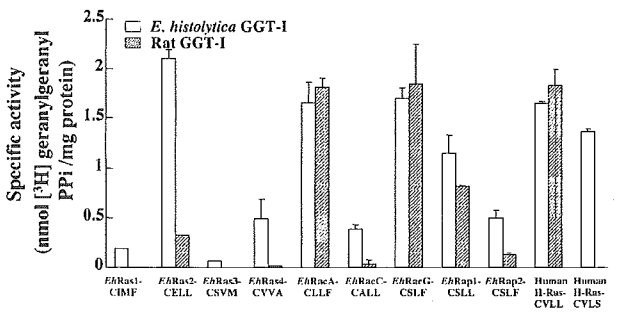

Fig. 4. Protein substrate specificity of recombinant GGT-I of *E. histolytica*. The specific activity of the recombinant *Eh*GGT-I was determined by the incorporation of [^{3}H] geranylgeranyl pyrophosphate into the recombinant *Eh*Ras1-4, *Eh*Rac A, C, G, *Eh*Rapl, 2, wild-type H-Ras-CVLS, and mutant H-Ras-CVLL. The reaction mixture (50 μl) contained 50 mM HEPES, pH 7.5, 5 mM $MgCl_2$, 25 μM $ZnCl_2$, 5 mM DTT, 0.1% PEG 20,000, 130 nM [^{3}H] GGPP (3 μCi/ml), 1.8 μg (1.8 μM) of an acceptor, and 2.4 μg (0.6 μM) of the purified recombinant GGT-I. Means ± standard errors of quadruplicates are shown. DDBJ/EMBL/GeneBank™ accession numbers of these proteins are: *Eh*Rasl, AAA21446; *Eh*Ras2, AAA21447; *Eh*Ras3, BAD07406; *Eh*Ras4, BAB07407; *Eh*RacA, Q24814; *Eh*RacC, Q24816; *Eh*RacG, O76321; *Eh*Rapl, AAA21444; *Eh*Rap2, AAA21445; H-Ras-CVLS, P01112.

We examined the specificity of the prenyl donors of *Eh*GGT-I and rat GGT-I. The recombinant *Eh*GGT-I showed farnesyl transferase activity against *Eh*Ras2-CELL and H-Ras-CVLL at about 27% the efficiency of geranylgeranyltransferase. In contrast, rat GGT-I showed significantly lower FT activity against the same acceptors (3.3–6.6% of GGT-I activity) (data not shown).

3.5. Kinetic properties of EhGGT-I

Lineweaver-Burk plots showed the K_m of recombinant *Eh*GGT-I for *Eh*Ras2 and H-Ras-CVLL to be 0.85 ± 0.11 and 0.2 ± 0.01 μM (plots not shown), respectively. The K_m of recombinant rat GGT-I for H-Ras-CVLL was 6 times higher (1.2 μM [41]), suggesting the higher substrate affinity of the amebic GGT-I toward protein acceptors. *Eh*GGT-I showed a K_m of 0.20 ± 0.05 μM for GGPP (using H-Ras-CVLL as a protein substrate), which is four times lower than that of rat GGT-I

Table 1
Inhibition of recombinant GGT-I from *Entamoeba histolytica* and rat by peptidomimetics

Inhibitors	IC_{50} (μM)			
	E. histolytica GGT-I		Rat GGT-I	
	*Eh*Ras2-CELL	H-Ras-CVLL	*Eh*Ras2-CELL	H-Ras-CVLL
GGTI-287	5.5 ± 1.8	25.3 ± 7.6	0.063 ± 0.004	0.049 ± 0.02
GGTI-297	3.2 ± 0.4	2.1 ± 0.3	0.033 ± 0.004	0.257 ± 0.03

The reaction mixture contained, in a total volume of 50 μl, 50 mM HEPES, pH 7.5, 5 mM $MgCl_2$, 25 μM $ZnCl_2$, 5 mM DTT, 0.1% PEG 20,000, 130 nM [^{3}H] GGPP (3 μCi/ml), 1.8 μg (1.8 μM) of the acceptor, and 2.4 μg (0.6 μM) of the recombinant GGT-I. IC_{50} of each peptidomimetics was determined by measuring specific activities with a range of 0.01–100 μM of the compounds.

(0.81 ± 0.27 μM). *Eh*GGT-I also showed a higher affinity for FPP than rat GGT-I; the K_m of *Eh*GGT-I or rat GGT-I for FPP using H-Ras-CVLL was 29.8 ± 3.7 or >400 nM, respectively.

3.6. Sensitivity of recombinant EhGGT-I to inhibitors of mammalian GGT-I

We examined the sensitivity of *Eh*GGT-I to known peptidomimetic GGT-I inhibitors. As shown in Table 1, *Eh*GGT-I was eight and 516 times more resistant to GGTI-287 than rat GGT-I when recombinant *Eh*Ras2-CELL and H-Ras-CVLL were used as substrates, respectively. *Eh*GGT-I was also 97 and eight times less sensitive to GGTI-297 than rat GGT-I, respectively.

4. Discussion

In this study, we demonstrated marked biochemical differences in the major prenyl enzyme responsible for the lipid modification of Ras and Rho/Rac small GTPases between the enteric protozoan parasite and its mammalian host. This study represents the first biochemical characterization of GGT-I from unicellular protozoa. Our genome-wide search of a GGT-Iβ gene among parasitic protozoa, together with the previous report on the lack of GGT-I activity in kinetoplastids [9], indicates that all protozoan parasites except for *E. histolytica* where the genome database is available lack GGT-I, reinforcing the peculiarity of *E. histolytica*, which possesses both FT and GGT-I. This apparent redundancy of the isoprenylation pathways may be associated with unique features of functions and regulations of Ras/Rap and Rho/Rac proteins through unusual lipid modifications in this parasite. It is totally unknown why *E. histolytica* mainly utilizes GGT-I for lipid modification of a majority of Ras/Rap and Rho/Rac and employs FT for isoprenylation of a very limited subset of Ras isotypes (solely *Eh*Ras4), while the other parasitic protists possess only FT and are likely to have lost GGT-I during parasitic or non-parasitic evolution.

Phylogenetic analyses indicate that *Eh*GGT-Iβ, as well as *Eh*GGT-Iα (*Eh*FTα) in our previous study [26], is only distantly associated with homologues from other organisms. This may partially explain why the unique biochemical properties of the amebic GGT-I that are not shared by its mammalian counterpart exist (see below). Our previous study suggested that α and β subunits of FT co-evolved at a comparable rate among organisms because the phylogenetic trees of the two FT subunits were almost identical [26]. However, the phylogenetic relationship of the β subunit of GGT-I is apparently distinct from that of α and β subunits of FT, refuting a hypothesis of the co-evolution of these two isoprenylation enzymes (Fig. 2).

The results of the GTPase substrate specificity of *Eh*GGT-I indicate that the Ras, Rac, and Rap proteins possessing CaaL, CaaF, CaaM, CaaA, or CaaS at the carboxyl terminus, either from *E. histolytica* or humans, can serve as acceptors for *Eh*GGT-I. Thus, the amebic GGT-I utilizes a broad range of small GTPases for geranylgeranylation. This is in striking contrast to the farnesylation of small GTPases by *Eh*FT, which showed an extremely limited substrate range; only *Eh*Ras4 can serve as a farnesyl acceptor. Our database analysis showed that *E. histolytica* Ras/Rap, Rho/Rac, and Rab with the CaaX terminus possess terminal Leu (42%), Phe (32%), Val (13%), Cys/Met (4% each), or Ala/Ser/Ile (2% each) (data not shown). In mammals, small GTPases with Leu and Val are exclusively geranylgeranylated by GGT-I, and those with Met, Gln, Ser, Ala, Thr, or Cys (in the order of frequency) are solely farnesylated by FT, while those with Phe are modified by both enzymes [42]. In contrast to the amebic GGT-I, mammalian GGT-I does not geranylgeranylate small GTPases with terminals Ala and Ser. Thus, the unique geranylgeranlylation of these small GTPases possessing terminal Ala or Ser in the ameba may confer a unique role to these GTPases. *E. histolytica* small GTPases with the CaaX terminus shows deviation toward Phe at the X position as shown above. However, amebic FT cannot utilize small GTPases terminating with Phe [26]. Taken together, this enteric protozoon strongly relies on GGT-I. It is conceivable that there are biological selections toward the current predominant utilization of GGT-I in this organism. For instance, since the farnesylation of CENP-E, a centromere-associated protein playing a critical role in cell cycle progression in mammals [43], is not present in *E. histolytica*, its modifying enzyme is not required because the isoprenylation of most of small GTPases, except for *Eh*Ras4, is accomplished by GGT-I and GGT-II (Rab GGT, Kumagai, M., Makioka, A., Takeuchi, T. and Nozaki, T., unpublished).

A comparison of ternary complexes of mammalian GGT-I and FT revealed that acceptor specificity is partially determined by surface complementarity between the X residue and the "specificity pocket," to which the side chain of the X residue binds [40]. For instance, the hydrophobic "specificity pocket" discriminates against polar side chains. In addition, the shape and volume of the "specificity pocket" further restrict the range of amino acids most preferably to Leu for GGT-I [40]. However, this preference for Leu was not observed for *Eh*GGT-I. It is intriguing that while the amebic GGT-I prefers *Eh*Ras2-CELL to the other three isotypes of *Eh*Ras possessing Phe, Met, or Ala at the carboxyl terminus (4–33 times in specific activity), it showed an opposite preference for Rac with carboxyl-terminal Phe (*Eh*RacA and *Eh*RacG) over Leu (*Eh*RacC). This observed discrepancy on the acceptor preference of the amebic GGT-I is not artifactual since FT revealed a reverse preference (i.e. approximately eight times higher activity against *Eh*Rasl than

*Eh*Ras2; [26]). These data suggest that the acceptor specificity of the amebic GGT-I is strongly influenced by neighboring residues of GGT-I other than the carboxyl terminus or tertial structure of small GTPases, which is remarkably different from mammalian GGT-I [42]. The data also indicate that the interaction between the surface of GGT-I and the upstream hyper variable region of small GTPases may differ between ameba and mammals. Although the carboxyl terminus of both *Eh*Rasl and *Eh*Ras2 is highly charged (the 17-a.a. carboxyl-terminal region contain nine or seven positively-charged and three or two negatively-charged amino acids in *Eh*Rasl or *Eh*Ras2, respectively), the total polarity of the carboxyl terminus of *Eh*Rasl is significantly higher than *Eh*Ras2. These changes may produce steric differences that lead to changes in substrate specificity. Note that the four substitutions among 12 residues implicated to bind a peptide substrate in mammalian GGT-Iβ [40] (Ala^{123} to Ser^{107}, Met^{124} to Tyr^{108}, Arg^{202} to Ser^{189}, and Leu^{320} to Met^{304}) in *Eh*GGT-Iβ result in the emergence of two hydroxyl-containing residues and the loss of one positive amino acid. The tertial structure of mammalian GGT-I revealed that Ala^{123} and Met^{124} in mammalian GGT-I do not directly interact with X residue of the protein substrate [42], but position close to the X residue. It is conceivable that substituting these amino acids with hydroxyl-containing Ser and aromatic Tyr, respectively, significantly influences the shape and charge of the end of the protein substrate-binding pocket, which likely results in the wider specificity of the amebic GGT-I for protein substrates.

*Eh*GGT-I also utilizes a wider range of isoprenyl donors. *Eh*GGT-I showed four to nine times higher farnesyltransferase activity than rat GGT-I. Five out of 17 residues implicated in the binding of isoprenoid in mammalian GGT-Iβ [40] are substituted in *Eh*GGT-Iβ (Fig. 1). Among these five substitutions (Phe^{52} to Met^{47}, Thr^{127} to Ala^{111}, Cys^{177} to Ser^{164}, Phe^{324} to Cys^{308}, and Asn^{345} to Ile^{329}) in *Eh*GGT-Iβ, Phe^{324} to Cys^{308} is worth noting. Phe^{324} of rat GGT-Iβ is in close proximity to the end of the C20 geranylgeranyl chain and is partially responsible, together with Thr^{49} (also conserved in *Eh*GGT-Iβ), for allowing rat GGT-I to accommodate GGPP in the catalytic pocket [40]. It is conceivable that Phe^{324} to Cys^{308} substitution creates additional water-mediated or non-mediated hydrogen bonds with neighboring residues, which result in the ability of *Eh*GGT-Iβ to utilize FPP as well as GGPP. This substitution may also influence the stability of the enzyme-product complex and the binding of fresh isoprenoid diphosphate to displace the prenyl-peptide product from the active site during the reaction cycle, as shown for rat GGT-I [40].

The amebic GGT-I revealed notable resistance to peptidomimetics known to inhibit mammalian GGT-I (Table 1). This apparent insensitivity of the amebic GGT-I to the inhibitors is not due to the impurity of our preparations since mixing our recombinant GGT-I with rat GGT-I did not influence the inhibition of rat GGT-I by these peptidemimetics. In addition, both amebic and rat GGT-I revealed comparable sensitivity against a GGPP derivative, 3-aza-2,3-dihydro-la-homo-GGPP (kindly donated by Prof. R.M. Coates, University of Illinois) (IC_{50}, approximately 4–10 μM), confirming the observed insensitivity of *Eh*GGT-I against GGTI-287 and GGTI-297. GGTI-287 and GGTI-297 are CaaL peptidomimetics, where reduced C is linked to Leu by 2-phenyl-4-aminobenzoic acid or by 2-naphthyl-4-aminobenzoic acid [44–46]. It is puzzling why the amebic GGT-I is insensitive to these CaaL peptidomimetics because *Eh*GGT-I shows wide donor specificity as discussed above.

Together with our previous study [26], this study indicates that most small GTPases with the CaaX motif from *E. histolytica* are geranylgeranylated or farnesylated by GGT-I, but not farnesylated by FT, which significantly differs from mammals where Ras and Rho/Rac proteins with CaaX are either farnesylated by FT or geranylgeranylated by GGT-I at a comparable frequency [42]. Thus, GGT-I is biologically and physiologically very important for *E. histolytica*, making *Eh*GGT-I an attractive, rational target for the development of new chemotherapeutics against amebiasis.

Acknowledgements

The authors thank Naohiro Watanabe, Jikei, for his valuable discussion and Yumiko Saito-Nakano, NIID, for immunoblotting and her helpful discussion. We also thank Tomomi Yamashita, Jikei, for her technical assistance. This work was supported by a Grant for Precursory Research for Embryonic Science and Technology (PRESTO), Japan Science and Technology Agency to T.N., a Health Sciences Research Grant for Research on Emerging and Re-emerging Infectious Diseases from the Ministry of Health, Labor, and Welfare to A.M. and T.N., Grant-in-Aid for Scientific Research from the Ministry of Education, Culture, Sports, Science and Technology of Japan to A.M. (13670256) and T.N. (16044250, 16017307, 15590378), and a Grant for the Project to Promote Development of Anti-AIDS Pharmaceuticals from the Japan Health Sciences Foundation to T.N. The database search was conducted with the 9× *E. histolytica* genome database available at the Institute for Genomic Research (TIGR) and the Sanger Institute with financial support from the National Institute of Allergy and Infectious Diseases and The Wellcome Trust.

References

[1] Zhang FL, Casey PJ. Protein prenylation: molecular mechanisms and functional consequences. Annu Rev Biochem 1996;65:241–69.
[2] Takai Y, Kaibuchi K, Kikuchi A, Kawata M. Small GTP-binding proteins. Int Rev Cytol 1992;133:187–230.
[3] Boguski MS, McCormick F. Proteins regulating Ras and its relatives. Nature 1993;366:643–54.
[4] Casey PJ, Seabra MC. Protein prenyltransferases. J Biol Chem 1996;271:5289–92.
[5] Maurer-Stroh S, Washietl S, Eisenhaber F. Protein prenyltransferases. Genome Biol 2003;4(212):1–9.
[6] James GL, Goldstein JL, Brown MS. Polylysine and CVIM sequences of K-RasB dictate specificity of prenylation and confer resistance to benzodiazepine peptidomimetic in vitro. J Biol Chem 1995;270:6221–6.
[7] Cox A, Der CJ. Farnesyltransferase inhibitors and cancer treatment: targeting simply Ras? Biochem Biophys Acta 1997;1333:F51–71.
[8] Gibbs JB. Ras C-terminal processing enzymes-new drug targets? Cell 1991;65:1–4.
[9] Gelb MH, Van Voorhis WC, Buckner FS, et al. Protein farnesyl and *N*-myristoyl transferases: piggy-back medical chemistry targets for the

development of antitrypanosomatid and antimalarial therapeutics. Mol Biochem Parasitol 2003;126:155–63.
[10] Sebti SM, Hamilton AD. Farnesyltransferase and geranylgeranyltransferase I inhibitors and cancer therapy: lessons from mechanism and bench-to-bedside translational studies. Oncogene 2000;19:6584–93.
[11] Stark Jr WW, Blaskovich MA, Johnson BA, et al. Inhibiting geranylgeranylation blocks growth and promotes apoptosis in pulmonary vascular smooth muscle cells. Am J Physiol 1998;275:L55–63.
[12] World Health Organization. *Entamoeba* taxonomy, vol. 75. Bull World Health Organ; 1997. pp. 291–292.
[13] Shen P-S, Lohia A, Samuelson J. Molecular cloning of *ras* and *rap* genes from *Entamoeba histolytica*. Mol Biochem Parasitol 1994;64:111–20.
[14] Shen P-S, Sanford JC, Samuelson J. *Entamoeba histolytica*: isoprenylation of $p21^{ras}$ and $p21^{rap}$ in vitro. Exp Parasitol 1996;82:65–8.
[15] Lohia A, Samuelson J. Molecular cloning of a *rho* family gene of *Entamoeba histolytica*. Mol Biochem Parasitol 1993;58:177–80.
[16] Lohia A, Samuelson J. Heterogeneity of *Entamoeba histolytica rac* genes encoding $p21^{rac}$ homologues. Gene 1996;173:205–8.
[17] Ghosh SK, Samuelson J. Involvement of $p21^{racA}$, phosphoinositide 3-kinase, and vacuolar ATPase in phagocytosis of bacteria and erythrocytes by *Entamoeba histolytica*: suggestive evidence for coincidental evolution of amebic invasiveness. Infect Immun 1997;65:4243–9.
[18] Guillen N, Sansonetti P. Rac G, a small GTPase, regulates capping of surface receptors in *Entamoeba histolytica*. Arch Med Res 1997;28:129–31.
[19] Guillen N, Boquet P, Sansonetti P. The small GTP-binding protein RacG regulates uroid formation in the protozoan parasite *Entamoeba histolytica*. J Cell Sci 1998;111:1729–39.
[20] Temesvari LA, Harris EN, Stanley Jr SL, Cardelli JA. Early and late endosomal compartments of *Entamoeba histolytica* are enriched in cysteine proteases, acid phosphatase and several Ras-related Rab GTPases. Mol Biochem Parasitol 1999;103:225–41.
[21] Juarez P, Sanchez-Lopez R, Ramos MA, Stock RP, Alagon A. Rab8 as a molecular model of vesicular trafficking to investigate the latter steps of the secretory pathway in *Entamoeba histolytica*. Arch Med Res 2000;31:S157–9.
[22] Saito-Nakano Y, Nakazawa M, Shigeta Y, Takeuchi T, Nozaki T. Identification and characterization of genes encoding novel Rab proteins from *Entamoeba histolytica*. Mol Biochem Parasitol 2001;116:219–22.
[23] Saito-Nakano Y, Yasuda T, Nakada-Tsukui K, Leippe M, Nozaki T. Rab5-associated vacuoles play a unique role in phagocytosis of the enteric protozoan parasite *Entamoeba histolytica*. J Biol Chem 2004;279:49497–507.
[24] Rodriguez MA, Garcia-Perez RM, Garcia-Rivera G, et al. An *Entamoeba histolytica* Rab-like encoding gene and prote: function and cellular location. Mol Biochem Parasitol 2000;108:199–206.
[25] Loftus B, Anderson I, Davies R, et al. The genome of the protist parasite *Entamoeba histolytica*. Nature 2005;433:865–8.
[26] Kumagai M, Makioka A, Takeuchi T, Nozaki T. Molecular cloning and characterization of a protein farnesyltransferase from the enteric protozoan parasite *Entamoeba histolytica*. J Biol Chem 2004;279:2316–23.
[27] Diamond LS, Mattern CF, Bartgis IL. Viruses of *Entamoeba histolytica* I. Identification of transmissible virus-like agents. J Viol 1972;9:326–41.
[28] Diamond LS, Harlow DR, Cunnick CC. A new medium for the axenic cultivation of *Entamoeba histolytica* and other *Entamoeba*. Trans R Soc Trop Med Hyg 1978;72:431–2.
[29] Nozaki T, Asai T, Kobayashi S, et al. Molecular cloning and characterization of the genes encoding two isoforms of cysteine synthase in the enteric protozoan parasite *Entamoeba histolytica*. Mol Biochem Parasitol 1998;97:33–44.
[30] Higuchi R. Recombinant PCR. In: Innis MA, Gelfand DH, Shinsky JJ, White TJ, editors. PCR Protocols: A Guide to Methods and Applications. New York: Academic Press; 1990. p. 177–83.
[31] Omer CA, Diehl RE, Krai AM. Bacterial expression and purification of human protein prenyltransferases using epitope-tagged, translationally coupled systems. Meth Enzymol 1995;250:3–21.
[32] Bradford MM. A rapid and sensitive method for the quantitation of microgram quantities of protein utilizing the principle of protein-dye binding. Anal Biochem 1976;72:248–54.
[33] Thompson JD, Higgins DG, Gibson TJ. CLUSTAL W: improving the sensitivity of progressive multiple sequence alignment through sequence weighting, position-specific gap penalties and weight matrix choice. Nucleic Acids Res 1994;22:4673–80.
[34] Saitou N, Nei M. The neighbor-joining methods: a new method for reconstructing phylogenetic trees. Mol Biol Evol 1987;4:406–25.
[35] Page RD. TreeView: an application to display phylogenetic trees on personal computers. Comput Appl Biosci 1996;12:357–8.
[36] Felsenstein J. Confidence limits on phytogenies: an approach using the bootstrap. Evolution 1985;39:783–91.
[37] Sambrook J, Fritsch EF, Maniatis T. Molecular Cloning: A Laboratory Manual. Cold Spring Harbor, New York: Cold Spring Harbor Laboratory Press; 1989.
[38] Pompliano DL, Rands E, Schaber MD, Mosser SD, Anthony NJ, Gibbs JB. Steady-state kinetic mechanism of Ras farnesyl:protein transferase. Biochemistry 1992;31:3800–7.
[39] Boguski MS, Murray AW, Powers S. Novel repetitive sequence motifs in the α and β subunits of prenyl-protein transferases and homology of the a subunit to the MAD2 gene product of yeast. New Biologist 1992;4:408–11.
[40] Taylor JS, Reid TS, Terry KL, Casey PJ, Beese LS. Structure of mammalian protein geranylgeranyltransferase type-I. Embo J 2003;22:5063–74.
[41] Zhang FL, Moomaw JF, Casey PJ. Properties and kinetic mechanism of recombinant mammalian protein geranylgeranyltransferase type I. J Biol Chem 1994;269:23465–70.
[42] Reid TS, Terry KL, Casey PJ, Beese LS. Crystallographic analysis of caax prenyltransferases complexed with substrates defines rules of protein substrate selectivity. J Mol Biol 2004;343:417–33.
[43] Abrieu A, Kahana JA, Wood KW, Cleveland DW. CENP-E as an essential component of the mitotic checkpoint in vitro. Cell 2000;102:817–26.
[44] Lerner EC, Qian Y, Hamilton AD, Sebti SM. Disruption of oncogenic K-Ras4B processing and signaling by a potent geranylgeranyltransferase I inhibitor. J Biol Chem 1995;270:26770–3.
[45] McGuire TF, Qian Y, Vogt A, Hamilton AD, Sebti SM. Platelet-derived growth factor receptor tyrosine phosphorylation requires protein geranylgeranylation but not farnesylation. J Biol Chem 1996;271:27402–7.
[46] Qian Y, Vogt A, Vasudevan A, Sebti SM, Hamilton AD. Selective inhibition of type-I geranylgeranyltransferase in vitro and in whole cells by CAAL peptidomimetics. Bioorg Med Chem 1998;6:293–9.

Parasitol Res
DOI 10.1007/s00436-005-0025-7

ORIGINAL PAPER

Asao Makioka · Masahiro Kumagai · Seiki Kobayashi · Tsutomu Takeuchi

Effect of artificial gastrointestinal fluids on the excystation and metacystic development of *Entamoeba invadens*

Received: 5 May 2005 / Accepted: 20 September 2005

Abstract The effect of artificial gastric fluid (AGF), containing 0.5% pepsin and 0.6% hydrochloric acid, pH 1.8, in distilled water, on the excystation and metacystic development of *Entamoeba invadens* was examined. Excystation, which was assessed by counting the number of metacystic amoebae after inducing excystation, was enhanced by pretreatment of cysts with AGF for 30 to 60 min at 37°C but not 26°C. Longer exposure of cysts to AGF significantly reduced their viability. Significant enhancement of excystation was observed by pretreatment of cysts with distilled water only at 37°C. In addition, 0.6% hydrochloric acid had a comparable enhancing effect on excystation to AGF. Metacystic development, when determined by the number of nuclei in amoeba, was slightly enhanced by pretreatment with AGF. An artificial intestinal fluid (AIF), containing 1% pancreatin, 1% sodium bicarbonate, and 5% ox bile, pH 8.0, in distilled water, had a significant toxic effect on cysts, where 1% pancreatin had neither an enhancing effect on excystation nor a toxic effect on cysts, whereas 5% ox bile had a toxic effect on cysts. Pretreatment of cysts with AGF followed by AIF had a similar toxic effect on cysts to that by AIF only. These results suggest that gastric fluid but not intestinal fluid at 37°C contributes to enhancing excystation for *Entamoeba* infection.

A. Makioka (✉) · M. Kumagai
Department of Tropical Medicine,
Jikei University School of Medicine,
3-25-8 Nishi-shinbashi, Minato-ku,
Tokyo 105-8461, Japan
e-mail: makioka@jikei.ac.jp
Tel.: +81-3-34331111
Fax: +81-3-34314459

S. Kobayashi · T. Takeuchi
Department of Tropical Medicine and Parasitology,
Keio University School of Medicine,
35 Shinanomachi, Shinjuku-ku,
Tokyo 160-8582, Japan

Introduction

Following the ingestion of cysts in contaminated food or water, excystation and metacystic developments are essential for *Entamoeba* infection, and their processes have been described for *Entamoeba histolytica* (Dobell 1928; Cleveland and Sanders 1930). Since *E. histolytica* does not encyst efficiently in axenic cultures, *Entamoeba invadens*, a reptilian parasite, has been commonly accepted as a model for the study of encystation and excystation (López-Romero and Villagómez-Castro 1993; Eichinger 1997). Excystation is the process through which the whole organism escapes from the cyst through a minute perforation in the cyst wall. Metacystic development is the process in which a hatched metacystic amoeba with four nuclei divides to produce eight amoebulae, which grow to become trophozoites (Dobell 1928; Cleveland and Sanders 1930; Geiman and Ratcliffe 1936). The transfer of *E. invadens* cysts in an encystation medium to a growth medium induces in vitro excystation (McConnachie 1955; Rengpien and Bailey 1975; Garcia-Zapien et al. 1995; Makioka et al. 2002). Before excystation in the ileum, cysts are exposed to gastric fluid and then intestinal fluid during passage through the stomach and intestine. Although cysts are resistant to gastric fluid, there are no reports of the effect of gastrointestinal fluid on the excystation and metacystic development of *Entamoeba*. We examined the effect of artificial gastrointestinal fluid on these processes of *E. invadens*. Here, we report that artificial gastric fluid (AGF) enhances excystation but has little effect on metacystic development, while artificial intestinal fluid (AIF) had a significant toxic effect on cysts, which was due to the bile in the fluid.

Materials and methods

Trophozoites of *E.invadens* strain IP-1 were cultured in an axenic growth medium BI-S-33 (Diamond et al. 1978) at 26°C. To obtain cysts, trophozoites (5×10^5 cells/ml) were transferred to an encystation medium called 47% LG (LG is BI without glucose; Sanchez et al. 1994). After 3 days of incubation, the percentage of encystation reached 80% on

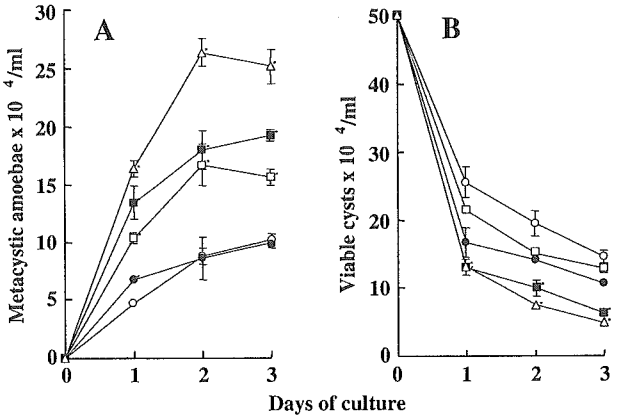

Fig. 1 Effect of AGF on the number of metacystic amoebae (**a**) and viable cysts (**b**) of *E. invadens*. The cysts were transferred to a growth medium without (*open circles*) or after pretreatment at 37°C with distilled water for 30 min (*filled circles*) or 60 min (*filled squares*) and with AGF for 30 min (*open squares*) or 60 min (*open triangles*). The mean numbers±SE of metacystic amoebae or viable cysts for duplicate cultures are plotted (each *asterisk* indicates $P<0.05$)

average. The cells were harvested and treated with 0.05% sarkosyl (Sigma Chemical Co., St. Louis, MO, USA) to destroy the trophozoites (Sanchez et al. 1994). The remaining cysts were washed with phosphate-buffered saline and counted. The viability of the cysts was determined by trypan blue dye exclusion, and the number of nuclei per cyst was determined after staining with modified Kohn's stain (Kumagai et al. 2001). Cyst preparation included 30% dead or denatured cysts and 70% viable cysts, where four-nucleate cysts are 30% and one- to three-nucleate cysts are 70%. For the experiments on excystation, cysts (5×10^5 cells/ml) in duplicate were suspended in a growth medium and were incubated for 3 days in the controls. For the experiments on the effect of AGF containing 0.5% pepsin (Nacalai Tesque, Kyoto, Japan) and 0.6% hydrochloric acid, pH 1.8, in distilled water on excystation, cysts were exposed to AGF for 30 or 60 min at 37°C, washed twice in the growth medium by centrifugation, and then suspended in a fresh growth medium, unless otherwise specified. Metacystic amoebae were counted in a hemocytometer on days 1 and 3, and their viability was determined by trypan blue dye exclusion. Viable metacystic amoebae and cysts were clearly distinguished as pale yellow and light blue in color, respectively. The former was also identified by positive motility. Metacystic development was determined by the number of nuclei per amoeba. The cells were harvested on days 1 and 3 in cultures and stained with modified Kohn's stain. The number of nuclei per amoeba was determined by the double counting of least 100 amoebae. A solution containing 1% pancreatin (Nacalai), 1% sodium bicarbonate, and 5% ox bile (Sigma), pH 8.0, in distilled water was used as the AIF (Heath and Smith 1970). For the experiments on the effect of AIF on excystation, the cysts were exposed to AIF for 60 min at 37°C, washed twice in a growth medium by centrifugation, and suspended in a fresh growth medium. For the combined effect of AGF and AIF on excystation, the cysts were exposed first to AGF for 60 min at 37°C, sedimented by centrifugation to remove AGF, and then exposed to AIF for 60 min at 37°C before transfer to the growth medium.

All experiments were performed at least three times, and similar results were obtained in each replicate. Therefore, representative data from duplicate cultures are shown in the results.

Results and discussion

Effect of AGF on excystation and viability of cysts

The effect of pretreatment of cysts with AGF on the number of metacystic amoebae and viable cysts of *E. invadens* before transfer to the growth medium is shown in Fig. 1a. The number of metacystic amoebae in cultures of cysts pretreated for 30 min with AGF during incubation increased compared to the controls. Pretreatment with distilled water for 30 min also increased the number of amoebae compared to the controls. When the pretreatment was increased from 30 to 60 min, metacystic amoebae further increased in number by pretreatment with AGF and distilled water. The effect of AGF on cyst viability is shown in Fig. 1b. The number of viable cysts in the control cultures decreased during incubation. It is considered that most immature cysts contained in culture degenerate or die

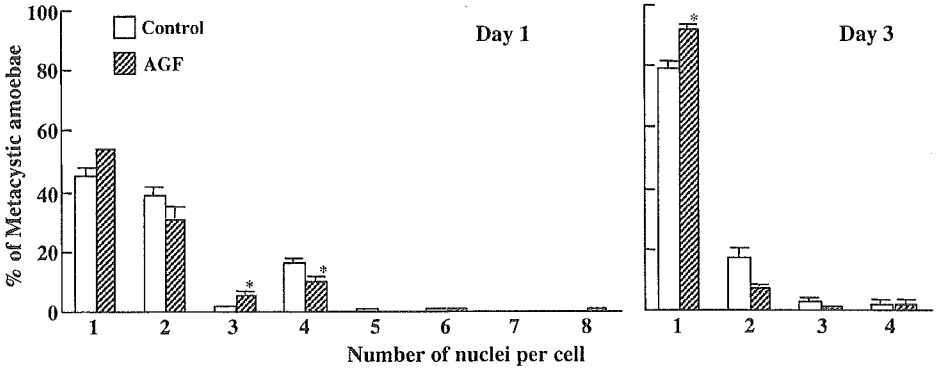

Fig. 2 Effect of AGF on the metacystic development of *E. invadens*. The cysts were transferred to a growth medium without or after pretreatment at 37°C with AGF for 60 min. The number of nuclei per metacystic amoeba stained with modified Kohn on days 1 and 3 of incubation was counted, and the percentage of amoebae in each class (1- to 8-nucleate) was determined (each *asterisk* indicates $P<0.05$)

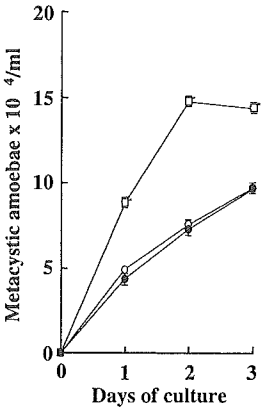

Fig. 3 Effect of temperature of pretreatment on the number of metacystic amoebae of *E. invadens*. The cysts were transferred to a growth medium without (*open circles*) or after pretreatment at 26°C (*filled circles*) or 37°C (*open squares*) with AGF for 60 min. The mean numbers±SE of metacystic amoebae for duplicate cultures are plotted (each *asterisk* indicates $P<0.05$)

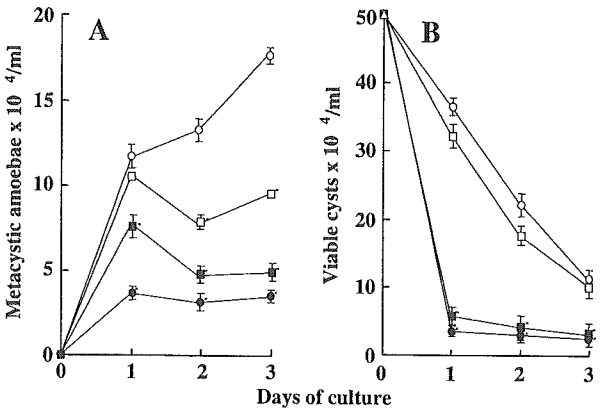

Fig. 5 Effect of AIF on the number of metacystic amoebae (**a**) and viable cysts (**b**) of *E. invadens*. The cysts were transferred to a growth medium without (*open circles*) or after pretreatment with AIF (*filled circles*), 1% pancreatin (*open squares*), or 5% bile (*filled squares*) for 60 min at 37°C. The mean numbers±SE of metacystic amoebae and viable cysts for duplicate cultures are plotted (each *asterisk* indicates $P<0.05$)

during incubation. The number of viable cysts in cultures of cysts pretreated with AGF or distilled water for 30 min during incubation was comparable to that of the controls, whereas pretreatment with AGF for 60 min reduced the number of viable cysts compared to the controls. This suggests that longer exposure to AGF had a detrimental effect on the cysts.

Effect of AGF on metacystic development

The effect of AGF on metacystic development was examined by counting the number of nuclei per cell. As shown in Fig. 2, 16 and 83% of the metacystic amoebae were four-nucleate and one- to three-nucleate, respectively, on day 1 of incubation in the control cultures, whereas 11 and 89% of amoebae, respectively, were in cultures of cysts pretreated with AGF. The percentage of four-nucleate amoebae in the control cultures then decreased to 2%, and that of 1-nucleate amoeba increased to 79% on day 3, while the percentages were 2 and 92%, respectively, in cultures of cysts pretreated with AGF, suggesting a small enhancing effect on metacystic development by pretreatment with AGF.

Effect of temperature of pretreatment with AGF on excystation

The effect of temperature of pretreatment with AGF on excystation is shown in Fig. 3. No increase in the number of metacystic amoebae by pretreatment of cysts with AGF at 26°C occurred, unlike at 37°C, indicating that a higher temperature of 37°C is critical for this effect. The results can be applied to excystation of the human parasite, *E. histolytica*, but are unlikely to be applicable to that of *E. invadens* in reptiles. Although encystation and excystation of *E. invadens* are important as models of encystation and excystation of *E. histolytica*, the difference in temperature for the axenic growth of the two species is definitive so that it is unlikely that temperature plays an important role in the in vivo excystation of *E. invadens*.

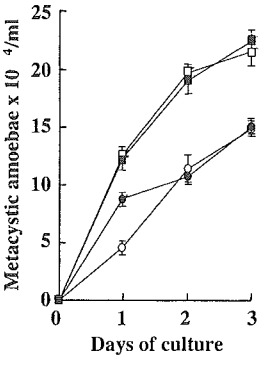

Fig. 4 Comparison of effect of pepsin, hydrochloric acid, and AGF on the number of metacystic amoebae of *E. invadens*. The cysts were transferred to a growth medium without (*open circles*) or after pretreatment for 60 min at 37°C with 0.5% pepsin in distilled water (*filled-circles*), 0.6% hydrochloric acid (*open squares*), or AGF (*filled squares*). The mean numbers± SE of metacystic amoebae for duplicate cultures are plotted (each *asterisk* indicates $P<0.05$)

Comparison of effect of pepsin, hydrochloric acid, and AGF on excystation

The effect of pepsin in distilled water, hydrochloric acid, and AGF on excystation was compared. As shown in Fig. 4, the increase in the number of metacystic amoebae by pretreatment with 0.6% hydrochloric acid was very similar to that

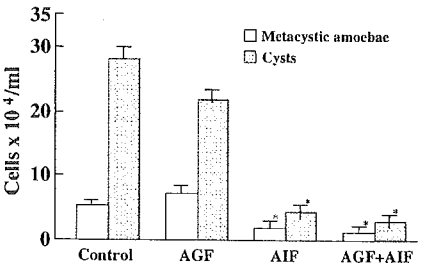

Fig. 6 Combined effect of AGF and AIF on the number of metacystic amoebae and viable cysts. The cysts were transferred to a growth medium without or after pretreatment with AGF or with AGF + AIF. The mean numbers±SE of metacystic amoebae and viable cysts on day 1 for duplicate cultures are plotted (each *asterisk* indicates $P<0.05$)

with AGF compared to the controls, whereas the increase occurred to a lesser extent only on day 1 by pretreatment with 0.5% pepsin in distilled water. This suggests that acidic conditions are important for the enhancing effect on excystation. Similar results were reported on *Giardia* in which excystation of this parasite could be induced by acidic solutions and also that salts and pepsin did not significantly alter the level of excystation in these solutions (Bingham and Meyer 1979). The mechanism for induction of *Giardia* and *Entamoeba* excystation by acidic conditions is unclear.

Effect of AIF on excystation and viability of cysts

The effect of pretreatment of cysts with AIF on the number of metacystic amoebae and viable cysts is shown in Fig. 5. Pretreatment of cysts with AIF for 60 min at 37°C significantly reduced the number of viable cysts, and few metacystic amoebae appeared. Similar results were obtained with exposure to AIF for 30 min (data not shown). When the effect of 1% pancreatin was compared with that of 5% ox bile, pancreatin showed neither an enhancing effect nor a toxic effect on cysts, whereas ox bile showed a toxic effect on cysts, indicating that the toxic effect on cysts by AIF was due to the bile.

Combined effect of AGF and AIF on excystation and viability of cysts

The effect of AGF and AIF on the number of metacystic amoebae and viable cysts on day 1 of incubation is shown in Fig. 6. Exposure of cysts to AGF and AIF resulted in a significant reduction in the number of viable cysts and little emergence of metacystic amoebae, which was similar to the results of AIF only.

In summary, these results suggest that gastric fluid but not intestinal fluid at 37°C contributes to enhancing excystation for *Entamoeba* infection.

Acknowledgements We thank Dr. N. Watanabe for valuable discussion, Dr. L.S. Diamond for supplying the *E. invadens*, and T. Tadano for technical assistance. This work was supported by a Grant-in-Aid for Scientific Research from the Ministry of Education, Culture, Sports and Technology of Japan and by a Health Science Research Grant for Research on Emerging and Re-emerging Infectious Diseases from the Ministry of Health, Labor and Welfare of Japan.

References

Bingham AK, Meyer EA (1979) *Giardia* excystation can be induced in vitro in acidic solutions. Nature 277:301–302

Cleveland LR, Sanders EP (1930) Encystation, multiple fission without encystment, excystation, metacystic development, and variation in a pure line and nine strains of *Entamoeba histolytica*. Arch Protistenkd 70:223–266

Diamond LS, Harlow DR, Cunnick CC (1978) A new medium for the axenic cultivation of *Entamoeba histolytica* and other *Entamoeba*. Trans R Soc Trop Med Hyg 72:431–432

Dobell C (1928) Researches on the intestinal protozoa of monkeys and man. Parasitology 20:357–412

Eichinger D (1997) Encystation of *Entamoeba* parasites. Bioessays 19:633–639

Garcia-Zapien A, Hernandez-Gutierrez R, Mora-Galindo J (1995) Simultaneous growth and mass encystation of *Entamoeba invadens* under axenic conditions. Arch Med Res 26:257–262

Geiman QM, Ratcliffe HL (1936) Morphology and life-cycle of an amoeba producing amoebiasis in reptiles. Parasitology 28:208–230

Heath DD, Smith JD (1970) In vitro cultivation of *Echinococcus granulosus*, *Taenia hydatigena*, *T. pisiformis* and *T. serialis* from oncosphere to cystic larva. Parasitology 61:329–343

Kumagai M, Kobayashi S, Okita T, Ohtomo H (2001) Modifications of Kohn's chlorazol black E staining and Wheatley's trichrome staining for temporary wet mount and permanent preparation of *Entamoeba histolytica*. J Parasitol 87:701–704

López-Romero E, Villagómez-Castro JC (1993) Encystation in *Entamoeba invadens*. Parasitol Today 9:225–227

Makioka A, Kumagai M, Ohtomo H, Kobayashi S, Takeuchi T (2002) Effect of proteasome inhibitors on the growth, encystation, and excystation of *Entamoeba histolytica* and *Entamoeba invadens*. Parasitol Res 88:454–459

McConnachie EW (1955) Studies on *Entamoeba invadens* Rodhain, 1934, in vitro, and its relationship to some other species of *Entamoeba*. Parasitology 45:452–481

Rengpien S, Bailey GB (1975) Differentiation of *Entamoeba*: a new medium and optimal conditions for axenic encystation of *E. invadens*. J Parasitol 61:24–30

Sanchez L, Enea V, Eichinger D (1994) Identification of a developmentally regulated transcript expressed during encystation of *Entamoeba invadens*. Mol Biochem Parasitol 67:125–135

EUKARYOTIC CELL, Apr. 2005, p. 722–732 Vol. 4, No. 4
1535-9778/05/$08.00+0 doi:10.1128/EC.4.4.722–732.2005

Identification and Gene Expression Analysis of a Large Family of Transmembrane Kinases Related to the Gal/GalNAc Lectin in *Entamoeba histolytica*†

David L. Beck,[1]‡ Douglas R. Boettner,[1] Bojan Dragulev,[1] Kim Ready,[2,3] Tomoyoshi Nozaki,[4,5] and William A. Petri, Jr.[1,2,3]*

Departments of Microbiology,[1] Medicine,[2] and Pathology,[3] University of Virginia, Charlottesville, Virginia 22908-1340, and Department of Parasitology, National Institute of Infectious Diseases, Tokyo 162-8640,[4] and Precursory Research for Embryonic Science and Technology, Japan Science and Technology Agency, 2-20-5 Akebonocho, Tachikawa, Tokyo 190-0012,[5] Japan

Received 22 November 2004/Accepted 9 February 2005

We identified in the *Entamoeba histolytica* genome a family of over 80 putative transmembrane kinases (TMKs). The TMK extracellular domains had significant similarity to the intermediate subunit (Igl) of the parasite Gal/GalNAc lectin. The closest homolog to the *E. histolytica* TMK kinase domain was a cytoplasmic dual-specificity kinase, SplA, from *Dictyostelium discoideum*. Sequence analysis of the TMK family demonstrated similarities to both serine/threonine and tyrosine kinases. TMK genes from each of six phylogenetic groups were expressed as mRNA in trophozoites, as assessed by spotted oligoarray and real-time PCR assays, suggesting nonredundant functions of the TMK groups for sensing and responding to extracellular stimuli. Additionally, we observed changes in the expression profile of the TMKs in continuous culture. Antisera produced against the conserved kinase domain identified proteins of the expected molecular masses of the expressed TMKs. Confocal microscopy with anti-TMK kinase antibodies revealed a focal distribution of the TMKs on the cytoplasmic face of the trophozoite plasma membrane. We conclude that *E. histolytica* expresses members of each subgroup of TMKs. The presence of multiple receptor kinases in the plasma membrane offers for the first time a potential explanation of the ability of the parasite to respond to the changing environment of the host.

The Gal/GalNAc lectin of *Entamoeba histolytica* mediates parasite adherence to the host and signals the initiation of cytolysis (41, 44, 45, 49). It is a heterotrimer consisting of covalently linked heavy (Hgl) and light (Lgl) subunits with a noncovalently linked intermediate (Igl) subunit (9, 36, 37, 43, 46). The Igl subunit of the Gal/GalNAc lectin has two known family members, Igl1 and Igl2. The Igl subunit has sequence similarity to the variant surface protein (VSP) of *Giardia*. We have previously identified a large number of proteins in the genome of *E. histolytica* containing CXXC motifs similar to those of Igl (8). Here we show that these CXXC-rich proteins form a large family of *E. histolytica* transmembrane kinases (TMKs) with highly variable extracellular domains homologous to Igl and VSPs of *Giardia* and with cytoplasmic kinase domains.

Amebic trophozoites have been demonstrated to persist in humans for longer than 6 months (21, 22). This prolonged period of infection suggests that the amebae evade the immune system. Other protozoan parasites, such as *Plasmodium*, *Giardia*, and *Trypanosoma brucei*, are also able to infect the host for long periods in spite of inducing robust immune responses. The mechanism(s) of persistence of these organisms is thought in part to be due to the variation of surface proteins. *Plasmodium falciparum* has three families of *var* genes that are independently expressed (29). The highest variation rate of these families is 2% per generation (52). *Giardia* encodes a family of 100 to 150 VSPs whose surface expression changes at a rate of one variation every 5 to 13 generations (38). *T. brucei* has a family of over 1,000 variant surface glycoproteins that change at a rate of 10^{-2} to 10^{-7} variations per generation (13, 51).

The discovery of the large family of CXXC-containing TMKs is of interest not only for their potential role in antigenic variation but also for their role in cell signaling. *E. histolytica* must respond to a wide variety of environmental stimuli as it excysts into a trophozoite in the intestinal lumen and enters the host by invasion of the intestinal mucosal epithelium. Invasion involves attaching to the epithelium and responding to that attachment event through signaling events via the *E. histolytica* Gal/GalNAc adherence lectin that lead to host cell killing. The changing host environment should necessitate having a variety of ways of sensing and responding to the host.

Here we report sequence and expression analysis of the TMKs in laboratory-cultured trophozoites. An oligoarray and real-time PCR were used to measure the expression in cultured trophozoites of the TMK genes. We demonstrate that there are six families of TMKs, with each having one or more family members expressed. In addition, anti-TMK antibodies

* Corresponding author. Mailing address: Division of Infectious Diseases, P.O. Box 801340, Rm. 2115, MR4 Bldg., University of Virginia Health System, Charlottesville, VA 22908-1340. Phone: (434) 924-5621. Fax: (434) 924-0075. E-mail: wap3g@virginia.edu.

‡ Present address: Department of Biology and Chemistry, Texas A&M International University, 5201 University Blvd., Laredo, TX 78041-1900.

† Supplemental material for this article may be found at http://ec.asm.org/.

were used to localize the TMKs to the plasma membrane of trophozoites, consistent with their proposed function in sensing the environment.

MATERIALS AND METHODS

Identification of genes homologous to the Igl subunit of the Gal/GalNAc lectin. The genes were identified in the 7X assembly available from The Institute for Genomic Research (TIGR) and Sanger sequencing centers (http://www.tigr.org/tdb/e2k1/eha1 and http://www.sanger.ac.uk/Projects/E_histolytica/) by searching the database for homologs of Igl1. Genes with high sequence similarity to Igl1 were used to search the database and identify additional family members. Additionally, the Sanger assembly was translated in all six reading frames, and genes were identified by sequence similarity to known genes in the National Center for Biotechnology Information (NCBI) database. These sequences were then screened for genes containing sequences for three or more CXXC motifs, or kinase domains. Genes containing sequences for CXXC motifs but not kinase domains, transmembrane domains, or signal peptides were eliminated from the data set.

Identification of other virulence genes and control genes. Genes were identified by sequence similarity to genes for amoebapores, cysteine proteinases, and the Gal/GalNAc lectin Igl, Lgl, and Hgl subunits. Additionally, genes were identified by examination of the translated Sanger assembly, which had been annotated to known genes in the NCBI database. Phagocytosis genes and control genes were similarly identified. BspA genes were identified in the translated Sanger assembly and then identified by sequence similarity in the TIGR assembly.

Phylogenetic analysis of the TMK proteins. A 260-amino-acid alignment of the kinase domains of the TMK proteins was made to Hanks's kinase alignment (Protein Kinase Resource [http://pkr.sdsc.edu/html/pk_classification/pk_catalytic/pk_hanks_class.html]) using CLUSTALX (20, 61). One representative per family, called the query panel of kinases, was employed (http://pkr.sdsc.edu/html/pk_classification/pk_catalytic/query_panel.html). The alignment was manually optimized using Genedoc (39), and then sequences were analyzed using the PHYLIP v3.6 package (15) and bootstrapped using Seqboot, Protdist, Neighbor, and Consense. A subset of the sequences were then bootstrapped using Seqboot, Protpars, and Consense. The TMKs were broken into groups based on signature motifs found in the kinase domains and aligned using CLUSTALX and with manual adjustments using Genedoc.

Probes for microarray analysis. Oligonucleotide probes typically ranging from 50 to 60 bases, and optimized for standard hybridization conditions, were designed using Array Designer 2.0 software (Premier Biosoft International, Palo Alto, CA). The selected probes were then analyzed by BLAST against the 7X assembly of the *E. histolytica* genome at both TIGR and Sanger. Probes were redesigned if they contained more than 75% sequence similarity with other target sequences or had a continuous stretch of complementary sequence exceeding 15 bases (28). In some cases it was not possible to design gene-specific probes. The actin probe was predicted to hybridize to several actin genes, the Jacob probe to all three Jacob genes, the EHCP1/2 probe to genes for both *E. histolytica* cysteine proteases 1 and 2 (EHCP1 and EHCP2), the Hgl family probes to all five Hgl genes but not homolog Sp1, and the Hgl1/5 probe to Hgl1 and Hgl5 genes. The Hgl1/5, Hgl2, Hgl3, and Hgl4 probes were more than 75% similar.

The oligoarray had probes to genes for amoebapores A, B, and C and homologs (32, 67), BspA homologs (25), actin, intergenic regions, L37a from mouse and human, chitin synthase (10), chitinase (11), Jacob (16), Jessie1-3 (65), EHCPs (6), EhRabs (53, 54), Vps26, Vps35, glycerate dehydrogenase (3), methionine gamma-lyase (62), phosphoglycerate dehydrogenase (2), Ebp1 and Ebp2 (55), L10 (7), ribosomal gene 8a, indigoidine synthase homolog (50), Hgl1-5 (35, 48, 58), Igl1 and Igl2 (8), Lgl1-6 (36, 59), Sp1 (an Hgl homolog), ferredoxin (26), Ariel1 (34), an HMW1 homolog (19), serine-rich *E. histolytica* protein (56), TMK genes, and other hypothetical surface genes (Table S1 in the supplemental material). TMK genes for which we did not generate a specific probe are shown in Table S2. Jacob is an amebic cyst wall glycoprotein expressed during encystation (16). EHCP1 and EHCP2 are highly homologous cysteine proteinases (6). Sp1 is a homolog of Hgl, recently identified in the TIGR database (B. Mann, personal communication).

Probe synthesis and microarray printing. A 200-nmol quantity of each probe (typically ranging from 50 to 60 bases optimized for standard hybridization conditions) was synthesized on an ABI 3900 DNA synthesizer (Applied Biosystems, Foster City, CA). The probe oligonucleotides were dissolved in 50% dimethyl sulfoxide at a concentration of 0.25 mg/ml and arranged in 96-well microtiter plates. The panel of probes, including control (housekeeping) oligonucleotides, was printed with two spot replicates on Corning UltraGAPS coated slides using an Affymetrix 417 arrayer (Affymetrix, Santa Clara, CA). Slide quality control was analyzed by hybridizing two randomly selected slides per batch (up to 40 slides/batch) with Cy3-labeled universal oligonucleotide probes. The hybridized slides were then washed and scanned with a ScanArray 4000 scanner (PerkinElmer Life Sciences Inc., Boston, MA). If the spotting quality standards were met, the batch was deemed satisfactory for analysis.

Ameba culture. Trophozoites of *E. histolytica* strain HM1:1MSS were grown axenically at 37°C in TYI-S-33 medium (12) with 100 U/ml of penicillin and 100 μg/ml of streptomycin sulfate (Invitrogen, Carlsbad, CA). For growth curve analysis, amebae were grown until they became nonadherent but still viable (144 h), seeded into T25 flasks with 300,000 ameba per flask (Corning Life Sciences, Corning, NY), and grown for 12 to 144 h.

Erythrophagocytosis. Human erythrocytes were isolated using Mono-Poly resolving medium (ICN Biomedicals, Aurora, OH) according to the manufacturer's directions. Erythrocytes were washed twice in 10 mM HEPES (pH 7.0), 140 mM sodium chloride, and 0.1% bovine serum albumin and then resuspended in the same buffer until use. One million log-phase trophozoites were grown in 50 ml of TYI-S-33 medium for 24 h in the presence or absence of 24 million erythrocytes per ml of medium.

Isolation of RNA. Amebae were lysed with 2 ml of buffer RLT containing β-mercaptoethanol (the first component of the RNeasy kit from Qiagen, Valencia, CA). Samples were processed immediately or flash-frozen in liquid nitrogen and stored at −80°C until processing using QIAshredders, followed by the RNeasy mini kit, including all optional steps and a 5-min incubation with buffer RWI. Samples were treated on the columns with RNase-free DNase from Qiagen according to the manufacturer's directions (Qiagen). Samples were analyzed for residual DNA contamination by PCR using primers for Jacob (conditions are described below). Samples that contained residual DNA were retreated with DNase I (Roche, Indianapolis, IN) for 1 h at 37°C in a 100-μl total volume with 10 μl of 10× DNase I buffer (100 μM Tris [pH 7.5], 25 mM $MgCl_2$ and 5 mM $CaCl_2$) and 3 μl DNase I, repurified on RNeasy columns and rescreened for residual DNA contamination. The Agilent BioAnalyzer (Agilent Technologies, Palo Alto, CA) was used to assess RNA quality. The results were inspected to ensure that both ribosomal peaks were intact and that no degradation had occurred. Acceptable 260/280 ratios ranged from 1.8 to 2.1.

Sample labeling, hybridization, and scanning. DNA oligoarray assay of gene expression used cohybridization of two fluorescently labeled cDNA targets, prepared from different samples. For routine oligoarray expression analysis, a previously described (24) indirect labeling procedure was used. Approximately 10 μg of RNA per sample and random hexamers were used for synthesis of cDNA containing amino-allyl-labeled nucleotides. The newly synthesized cDNA was then labeled by a covalent coupling of an appropriate cyanine fluor (CyDye postlabeling reactive dye pack; Amersham Biosciences Corp., Piscataway, NJ). In a typical oligoarray assay, the cDNA of one preparation (control) was labeled with Cy5, while the second cDNA (experiment) was labeled with Cy3. Both reactions were purified with a QIAquick PCR purification kit (Qiagen) for removal of the uncoupled dye. The labeling efficiencies of the purified target preparations were examined by spectrophotometry, as well as by calculations of the mass of cDNA and Cy5 or Cy3 dye incorporation. The nucleotide-to-dye molecular ratios were considered suitable for oligoarray experiments with a ratio of less then 50 nucleotides/dye molecule. Both targets were equalized based on the total amount of dyes incorporated before hybridization (24). The samples were mixed, dried by speed vac, and dissolved in hybridization buffer solution (50% formamide, 5x SSC [1× SSC is 0.15 M NaCl plus 0.015 M sodium citrate] and 0.1% sodium dodecyl sulfate [SDS]). The cDNA-containing hybridization solution was then denatured, applied to the oligoarray (prehybridized in 5x SSC, 0.1% SDS and 1% bovine serum albumin), and hybridized at 42°C for 18 h. Following 5-min washes in 2× SSC–0.1% SDS and in 0.1× SSC, the slide was scanned using a ScanArray 4000 scanner (PerkinElmer, Wellesley, MA). Both Cy5 and Cy3 images of one experiment were analyzed with QuantArray 3.0 microarray analysis software. Normalization to median between both channels was used.

RT-PCR primer design. Real-time PCR (RT-PCR) primers (Table 1) were designed using Beacon Designer 2.0 (Premier Biosoft International, Palo Alto, CA). RT-PCR primers and oligoarray probes were designed independently; thus, the PCR fragment and the oligoarray probe represented different regions of the same gene. Each primer was analyzed against the TIGR *E. histolytica* database, and any primer that had significant sequence similarity to multiple genes was rejected. Thus, both the forward and reverse primers were specific for one gene, except actin, Jacob, and Hgl, which detected all family members and/or alleles in the genome. Optimal annealing conditions (determined by gradient PCR) were

TABLE 1. RT-PCR primers

Gene product	Primer sequence		Annealing temp (°C)
	Forward	Reverse	
RNA Pol II	AAAGAAGGTGTTACTGTAGACGTAGGG	ATCTGAACGGACACGGACATGAC	66
RNA Pol II L	CTAATAAACCAAAGCCAATGGGATTCTCTC	GCTGGATTATATGGTGAAGGACCTGAAC	66
RNA Pol II 13	GTCCCGACTGTCATCAAATAATGCTTCC	ACACAGAAACTTGTTGGGTCTTCAGC	66
Jacob	CAAAGGAGTTCAAATGGGATGTGTTAG	TTATTTGGTGTAGGAGTTGGTAATGGG	66
Tmk 19	TTGTAGAAAGGATTGTATGTGTGAAGATGG	AGCACATCCTAAACAATCTGAACGATAC	66
Tmk 21	TTTGCTTTGGAAGTGGGACATATTGTAACG	TCCACGTTCCCCATTTCCATCCATTTC	66
Tmk 31	CCTTATGGATGTCTTCGTTGTATGACTGG	AGTTGAGTCATTAACCTTCATTCCAAATTCAC	66
Tmk 63	GCTGAAGGAACACCCACATACGG	AGAAATAATAGCCATCAGCACATGACAAAC	66
Tmk 65	TGTAGTTAATGGGTCAGGGTATAAG	GCTCGTTGTTCTTCAGACATAAG	64
Tmk 71	TGTTGAAGGAGAAAAGAAAATGAATGG	CTGGTTGAGAAGGATTATGTATAGAGTC	62
Tmk 75	ACTCTGTTATGACTTGGGAAGATCCTTATC	GGTTCATCACACCAACACTCACATATAAG	66
Tmk 79	CCTGATGTTTCTAATCTTGTTGGACTTC	GCAAGTTCAAGTTCCTGATGAGAATATC	66
Tmk 80	CGCCTTTAGCCCACCCTCTTTTATTG	ACTGTCTGTTGTTGATTCACTGTATCTTCTC	66
Tmk 96	AATGGGTGTGCTGTTTGTCA	AAGCAACACACTTCGCGTCT	64
Tmk 98	TCTGCTGAAGGGTCTGTGGGTTCTC	CGGCTTTGACGGGTGTTTGTGAATTATG	66
SA	ACTTGCTGCTCGTGTCATTGC	TTAGTGAATGATCCTGGTGTGAATCTTC	66
Actin	GCACTTGTTGTAGATAATGGATCAGGAATG	ACCCATACCAGCCATAACTGAAACG	62
Hgl	GGCGGATCCTGTGGTGGAGATTCTACA	CATCACCAACTGCTTGAA	59

used to ensure specificity, and any PCR primer pair that produced more than one melt peak was discarded. PCR products that produced single melt peaks were analyzed by gel electrophoresis in 1.5% agarose–Tris-borate-EDTA, and if multiple bands were observed, the primer pair was discarded. Finally, all PCR products were sequenced using the forward amplification primer to verify specificity.

Real-time PCR validation of oligoarray results. RNA was reverse transcribed using iQsuperscript (Bio-Rad, Hercules, CA) according to the manufacturer's directions. cDNA levels were measured using RiboGreen (Molecular Probes, Eugene, OR) with DNA of known quantity as a standard in a SPECTRAmax Gemini EM fluorescent plate reader, according to the manufacturer's directions. Before proceeding to analysis of cDNA samples, a no-reverse-transcriptase control PCR was done using primers to the cyst-specific gene Jacob to verify that there was no residual DNA contamination of the samples. All samples were analyzed in duplicate, and all time points were analyzed in triplicate. Each time point was thus represented in six wells during the real-time PCR assays, and the six wells were averaged after normalization to the RNA polymerase II gene's average (47). Two sequentially performed growth curves were analyzed in the real-time PCR assays to ensure reproducibility. All real-time PCR assays were quantitative to allow direct comparison of gene expression levels.

A PCR master mix consisted of 1,100 μl of iQSYBRGreen super mix (Bio-Rad, Hercules, CA), 1,100 μl of distilled H_2O, 88 μl of forward primer (50 pmol/μl), and 88 μl of reverse primer (50 pmol/μl). To each well containing 2 μl of cDNA was added 25 μl of master mix. Duplicate assays were performed on each sample. Each assay included standards, no-DNA-control wells, and no-RT-control wells. The cycling conditions were 95°C for 5 min; 30 cycles of 95°C for 30 s, annealing for 30 s (see Table 1 for annealing temperatures), and 72°C for 30 s; and 1 cycle of 72°C for 2 min 30 s followed by a 90-step melt curve increasing 0.2°C with a 5-s hold.

TABLE 2. Properties of the domains of the *E. histolytica* transmembrane kinase groups

Group[a]	Transmembrane kinase no.	Size[b]	No. of amino acids, TM to kinase[c]	Signature motif in kinase	No. of amino acids, kinase to end[d]	No. of motifs[e]			
						CXC	CXXC	CXXXC	CXXCXXGYY
A	4, 17, 23, 25, 52, 53, 55, 61, 65, 68, 69, 72, 85	517–532	220	CC(I/V)KITDFGTSR[f]	40	4	4/5	3/4	3
B1	5, 12, 43, 76, 86, 91, 95, 100, 101, 103, 104	897–916	135	KLTDFGS(A/S)R[g]	0	1	25	2	9
B2	2, 8, 10, 11, 14, 15, 31, 36, 41, 62, 74, 75, 77, 87, 88, 92, 94, 105	822–1762	133	KLTDFGS(A/S)R[h]	0	0	90	0	25
B3	21, 28, 29, 30, 32, 35, 37, 38, 42, 48, 51, 96	830–2117	145	KLTDFGS(A/S)R	0	0	24	0	7
C	9, 13, 39, 60, 63, 71	547–624	160	C(A/G)KLTDFGTC[i]	59–82	0	33	0	11
D1	3, 18, 40, 56, 70, 79	520–619	234	PITAKVTDFGTS	63	3	5	3	7
D2	19, 27, 44, 46, 50, 57, 64, 67, 82, 97, 98	399–614	233	V(T/V)(C/X)KV(T/S)DFGTS	55	4	5	3	9
E	22, 54, 66	401–412	150	AKLSDFGTSR	60–97	1	0	0	0
F	34, 45, 59, 80	231–368	24	VKVSDFGLS and WXAPE	0	0	0	0	0

[a] Group G transmembrane kinases are diverse and include kinases 1, 6, 16, 24, 47, 49, 73, 79, with no common signature motif or other features within the group or with other groups.

[b] Number of amino acid residues in the extracellular domain.

[c] Amino acids from the C terminus of the transmembrane domain to the N-terminal glycine of the kinase domain.

[d] Amino acids from 10 residues after the conserved arginine to the stop codon.

[e] Number of times each motif is found in the protein sequence. The number of CXC, CXXC, CXXXC, and CXXCXXGYY motifs may vary between individual family members. Values with a slash indicate that some family members have 4 or 5, or 3 or 4, of the motif.

[f] Group A TMKs can additionally be identified by a moderately conserved (K/R)XXXDI(E/N)I(Y/F)KQQQPXYYYYIXGSXXXPXKXX(K/R)Y motif C-terminal to the transmembrane domain.

[g] Group B1 TMKs can be identified by a KRKEKKEREKTTIFKTITQSNI(K/R)FI(S/P)LGDG sequence after their transmembrane domain.

[h] Group B2 TMKs can be identified by a PV(N/G)(Q/E/K)E(S/T)(K/R)DL(L/I)CIGNXXKXXXKVQ sequence after their transmembrane domain.

[i] Group C TMKs can be identified by a RRR(K/R)XXKXXXXXIKPF(H/K)VSSD(I/V)ELXLL sequence following the transmembrane domain.